

# SPECTRAL MEASURE COMPUTATIONS FOR COMPOSITE MATERIALS

N. B. MURPHY\*, E. CHERKAEV†, C. HOHENEGGER‡, AND K. M. GOLDEN§

University of Utah, Department of Mathematics  
155 S 1400 E RM 233, Salt Lake City, UT 84112-0090, USA

**Abstract.** The analytic continuation method of homogenization theory provides Stieltjes integral representations for the effective parameters of composite media. These representations involve the spectral measures of self-adjoint random operators which depend only on the composite geometry. On finite bond lattices, these random operators are represented by random matrices and the spectral measures are given explicitly in terms of their eigenvalues and eigenvectors. Here we provide the mathematical foundation for rigorous computation of spectral measures for such composite media, and develop a numerically efficient projection method to enable such computations. This is accomplished by providing a novel formulation of the analytic continuation method which is equivalent to the original formulation and holds for both the finite lattice setting and the infinite settings. We also introduce a family of random bond lattices and directly compute the associated spectral measures and effective parameters. The computed spectral measures are in excellent agreement with known theoretical results. The behavior of the associated effective parameters is consistent with the symmetries and theoretical predictions of models, and the computed values fall within rigorous bounds. Some previous calculations of spectral measures have relied on finding the boundary values of the imaginary part of the effective parameter in the complex plane. Our method instead relies on direct computation of the eigenvalues and eigenvectors, which enables, for example, statistical analysis of the spectral data.

**Key words.** composite materials, random resistor network, percolation, homogenization, spectral measure, random matrix

**subject classifications.** 00B15, 47B15, 65C60, 30B40, 78A48, 80M40, 60K35

**1. Introduction** Over the years a broad range of mathematical techniques have been developed that reduce the analysis of complex composite materials, with rapidly varying structures in space, to solving averaged, or *homogenized* equations involving an effective parameter. Homogenization for composite media with rapidly varying coefficients of thermal conductivity, electrical conductivity, electrical permittivity, or magnetic permeability, for example, was established by Papanicolaou and Varadhan [69] for the steady state, static case with real parameters [58]. This work was extended by Golden and Papanicolaou [34, 35] to the quasi-static frequency dependent case with complex parameters. Analysis of the effective dielectric problem for the fully frequency dependent case described by the Helmholtz equation is given in [75].

The analytic continuation method (ACM) of homogenization theory for *two-component* media in the quasi-static limit was developed by Bergman [7], Milton [55], and Golden and Papanicolaou [34], leading to Stieltjes integral representations for the effective parameters. The Golden-Papanicolaou formulation of this method is based on the spectral theorem and resolvent formulas involving random self-adjoint operators. This formulation demonstrated that the measures underlying these integral representations are *spectral measures* associated with the random operators, which depend only on the composite geometry. These measures contain all the information about the mixture geometry, and provide a link between microgeometry and

---

\*murphy@math.utah.edu

†elena@math.utah.edu

‡choheneg@math.utah.edu

§golden@math.utah.edu

transport. Local geometry is encoded in “geometric” resonances in the measures [47], while global connectivity is encoded by spectral gaps in the measures at the spectral endpoints [60, 47]. A remarkable feature of the method is that once the spectral measures are found for a given composite geometry, by the spectral coupling of the governing equations [13, 58, 14, 18], the effective electrical, magnetic, and thermal transport properties are *all* completely determined by these measures.

The integral representations yield rigorous *forward bounds* on the effective parameters of composites, given partial information on the microgeometry [7, 55, 34, 8, 10]. One can also use the integral representations to obtain inverse bounds, where data on the electromagnetic response of a sample, for example, is used to bound its structural parameters, such as the volume fractions of the components [53, 54, 16, 13, 17, 81, 9, 15, 21, 33], and even the separation of the inclusions in matrix particle composites [66]. Furthermore, the spectral measure can be *uniquely* reconstructed [13] when the data is given for a continuous interval of electromagnetic frequency. This, in turn, can be used to calculate other effective parameters, such as the viscoelastic modulus [15], effective thermal conductivity [14, 18], and recover the associated structural parameters [13, 17, 81, 9, 15, 21, 33]. For classes of composites which undergo a percolation transition [77, 80], the integral representations have been used to obtain detailed information regarding the critical behavior of the effective parameters in the scaling regime [31, 60]. The relationship between the effective parameters and the system energy [60] has also led to a physically consistent statistical mechanics model for two-component dielectric media which is also mathematically tractable [63].

Despite the many applications which have stemmed from the ACM, explicit analytical calculations of the effective parameters and spectral measures have been obtained for only a handful of composite microstructures. There are various numerical methods which have been used to compute the effective parameters of two-component composites. These computations may, in principle, be used to compute the corresponding spectral measures through the Stieltjes–Perron inversion theorem. This theorem states that the measure is recovered as a weak limit of the imaginary part of the effective parameter in the complex plane.

Highly accurate numerical computations of the effective permittivity for a class of continuum composites which have sharp corners are described in [42]. The computations are based on a multigrid recursive compressed inverse preconditioning method [43, 41, 40] developed for calculation of the effective conductivity of random checkerboards. In [20] the effective conductivity of the 2D random resistor network (RRN) was computed using an efficient algorithm that implements  $Y$ - $\Delta$  transformations of the network. In [37, 12, 36] the Fast Multipole Method was exploited to compute the electrostatic fields and the effective conductivity for two-component matrix particle composites.

In [42, 20], the spectral measures associated with the composite microstructures of interest were computed using the Stieltjes–Perron inversion theorem. However, the presence of delta components or essential singularities in the measures, for example, makes it difficult to resolve details of the spectrum using this approach. To help overcome this limitation, here we develop a mathematical framework which provides a rigorous way to directly compute the spectral measures and effective parameters for finite lattice composite microstructures, or discretizations of continuum composites. In particular, we provide a novel formulation of the ACM which is equivalent to the original formulation [34, 10] and holds for both the finite lattice setting and the infinite settings. This analysis demonstrates that, in the finite lattice setting, the ran-

dom operators underlying the integral representations of the effective parameters are represented by random matrices, and the spectral measures are determined explicitly by their eigenvalues and eigenvectors.

As a consequence, our approach provides a direct connection between the statistical behavior of spectral data of random matrices and the behavior of the effective transport processes of composites. This, in turn, has provided a direct connection between the ACM and random matrix theory, and has shown that transitions in the connectedness or percolation properties of composites are reflected in the short and long range eigenvalue correlations of the underlying random matrices [61]. Moreover, this transitional behavior is captured by a one parameter universality class of random matrix ensembles and provides a mechanism for the collapse of gaps in the spectral measures [61], which leads to critical behavior in the effective transport coefficients of composites [60]. This characterization of critical behavior of transport in composites by the statistical properties of eigenvalues and eigenvectors of random matrices is a key feature of the ACM and our computational approach.

**2. Mathematical Methods** We now formulate the effective parameter problem for random two-phase conductive media in the continuum and lattice settings, yielding Stieltjes integral representations for the effective conductivity and resistivity tensors. In Section 2.1, we review and extend the ACM for the continuum setting [34], while the lattice setting is discussed in Section 2.2. The mathematical framework underlying the *infinite* lattice setting [11, 29], reviewed in Section 2.2.1, is analogous to that of the continuum case [11], and the integral representations for the effective parameters follow with minor modifications in the theory. In Section 2.2.2, we develop a mathematical framework for the *finite* lattice setting, leading to integral representations for the effective parameters, summarized in Theorem 2.1, which are analogous to that of the infinite, continuum and lattice cases. In order to derive the integral representations for the finite lattice setting, significant modifications must be made to the underlying mathematical framework. Toward this goal, in Section 2.2.3 we provide a novel formulation of the ACM which unifies the infinite settings and the finite lattice setting. The proof of Theorem 2.1 is given in Section 2.2.4.

**2.1. Continuum Setting** Consider a random two-phase conductive medium filling all of  $\mathbb{R}^d$ , which is determined by the probability space  $(\Omega, P)$ . Here,  $\Omega$  is the set of all geometric realizations of our random medium, which is indexed by the parameter  $\omega \in \Omega$  representing one particular geometric realization, and  $P$  is the associated probability measure. Details regarding the underlying sigma-algebra are discussed in [69]. Let  $\sigma(\vec{x}, \omega)$  and  $\rho(\vec{x}, \omega)$ ,  $\vec{x} \in \mathbb{R}^d$ , be the local complex conductivity and resistivity tensors associated with the conductive medium, which are related by  $\sigma = \rho^{-1}$  and have components  $\sigma_{jk}(\vec{x}, \omega)$  and  $\rho_{jk}(\vec{x}, \omega)$ ,  $j, k = 1, \dots, d$ , that are (spatially) stationary random fields.

A *stationary* random field,  $f: \mathbb{R}^d \times \Omega \rightarrow \mathbb{C}$ , is a field such that the joint distribution of  $f(\vec{x}_1, \omega), \dots, f(\vec{x}_n, \omega)$  and that of  $f(\vec{x}_1 + \vec{\xi}, \omega), \dots, f(\vec{x}_n + \vec{\xi}, \omega)$  is the same for all  $\vec{\xi} \in \mathbb{R}^d$  and  $n \in \mathbb{N}$  [34, 69]. More specifically, we assume that there is a group of transformations  $\tau_x: \Omega \rightarrow \Omega$  and measurable functions  $f'(\omega) = f(0, \omega)$  on  $\Omega$  such that  $f(\vec{x}, \omega) = f'(\tau_{-x}\omega)$  for all  $\vec{x} \in \mathbb{R}^d$  and  $\omega \in \Omega$ , with  $\tau_x \tau_y = \tau_{x+y}$ . Moreover, we shall assume that the group is one-to-one and preserves the measure  $P$ , i.e.,  $P(\tau_x A) = P(A)$  for all  $P$ -measurable sets  $A$  [34, 69]. For notational simplicity, we will not distinguish between the functions  $f': \Omega \rightarrow \mathbb{C}$  and  $f: \mathbb{R}^d \times \Omega \rightarrow \mathbb{C}$ , as the context of each is now clear.

The group of transformations  $\tau_x$  acting on  $\Omega$  induces a group of operators  $T_x$  on the Hilbert space  $L^2(\Omega, P)$  defined by  $(T_x f)(\omega) = f(\tau_{-x}\omega)$  for all  $f \in L^2(\Omega, P)$ . Since  $\tau_x$  is measure preserving, the operators  $T_x$  form a unitary group and therefore have closed densely defined infinitesimal generators  $L_i$  in each direction  $i = 1, \dots, d$  with domain  $\mathcal{D}_i \subset L^2(\Omega, P)$  [34, 69]. Thus,

$$L_i = \left. \frac{\partial}{\partial x_i} T_x \right|_{x=0}, \quad i = 1, \dots, d, \quad (2.1)$$

where  $x_i$  is the  $i^{\text{th}}$  component of the vector  $\vec{x}$  and differentiation is defined in the sense of convergence in  $L^2(\Omega, P)$  for elements of  $\mathcal{D}_i$  [34]. The closed subset  $\mathcal{D} = \cap_{i=1}^d \mathcal{D}_i$  of  $L^2(\Omega, P)$  is a Hilbert space [34] with inner product  $\langle \cdot, \cdot \rangle_D$  given by  $\langle f, g \rangle_D = \langle f, g \rangle_{L^2} + \sum_{i=1}^d \langle L_i f, L_i g \rangle_{L^2}$ , where  $\langle \cdot, \cdot \rangle_{L^2}$  is the  $L^2(\Omega, P)$  inner product.

Consider the Hilbert space  $\mathcal{H} = \bigotimes_{i=1}^d L^2(\Omega, P)$  with inner product  $\langle \cdot, \cdot \rangle$  defined by  $\langle \vec{\xi}, \vec{\zeta} \rangle = \langle \vec{\xi} \cdot \vec{\zeta} \rangle$ , where  $\vec{\xi} \cdot \vec{\zeta} = \xi^\dagger \zeta$  denotes the dot-product on  $\mathbb{C}^d$  and  $\langle \cdot \rangle$  means ensemble average over  $\Omega$  or, by an ergodic theorem [34], spatial average over all of  $\mathbb{R}^d$ . Define the Hilbert spaces [34] of “curl free”  $\mathcal{H}_\times$  and “divergence free”  $\mathcal{H}_\bullet$  random fields

$$\begin{aligned} \mathcal{H}_\times &= \left\{ \vec{Y} \in \mathcal{H} \mid \vec{\nabla} \times \vec{Y} = 0 \text{ weakly and } \langle \vec{Y} \rangle = 0 \right\}, \\ \mathcal{H}_\bullet &= \left\{ \vec{Y} \in \mathcal{H} \mid \vec{\nabla} \cdot \vec{Y} = 0 \text{ weakly and } \langle \vec{Y} \rangle = 0 \right\}, \end{aligned} \quad (2.2)$$

where we have used the simplified notation  $\langle \vec{Y} \rangle = 0 \iff \langle Y_i \rangle = 0$  for all  $i = 1, \dots, d$ ,  $\vec{\nabla} \cdot \vec{Y} = \sum_{i=1}^d L_i Y_i$ , and  $\vec{\nabla} \times \vec{Y} = 0$  means  $L_i Y_j - L_j Y_i = 0$  for all  $i, j = 1, \dots, d$ . Consider the following variational problems [34]. Find  $\vec{E}_f \in \mathcal{H}_\times$  and  $\vec{J}_f \in \mathcal{H}_\bullet$  such that

$$\begin{aligned} \langle \sigma(\vec{E}_0 + \vec{E}_f) \cdot \vec{Y} \rangle &= 0 \quad \forall \vec{Y} \in \mathcal{H}_\times \\ \langle \rho(\vec{J}_0 + \vec{J}_f) \cdot \vec{Y} \rangle &= 0 \quad \forall \vec{Y} \in \mathcal{H}_\bullet, \end{aligned} \quad (2.3)$$

respectively. When the bilinear forms  $\Psi(\vec{\xi}, \vec{\zeta}) = \sigma \vec{\xi} \cdot \vec{\zeta}$  and  $\Phi(\vec{\xi}, \vec{\zeta}) = \rho \vec{\xi} \cdot \vec{\zeta}$  are bounded and coercive, these problems have unique solutions [34, 69] satisfying the quasi-static limit of Maxwell’s equations [46]

$$\begin{aligned} \vec{\nabla} \times \vec{E} &= 0, \quad \vec{\nabla} \cdot \vec{J} = 0, \quad \vec{J} = \sigma \vec{E}, \quad \langle \vec{E} \rangle = \vec{E}_0, \\ \vec{\nabla} \times \vec{E} &= 0, \quad \vec{\nabla} \cdot \vec{J} = 0, \quad \vec{E} = \rho \vec{J}, \quad \langle \vec{J} \rangle = \vec{J}_0. \end{aligned} \quad (2.4)$$

Here,  $\vec{E}(\vec{x}, \omega) = \vec{E}_0 + \vec{E}_f(\vec{x}, \omega)$  is the random electric field, where  $\vec{E}_f$  is the fluctuating field of mean zero about the (constant) average  $\vec{E}_0$ . Similarly,  $\vec{J}(\vec{x}, \omega) = \vec{J}_0 + \vec{J}_f(\vec{x}, \omega)$  is the random current density. Moreover, the components of  $\vec{E}_f$  and  $\vec{J}_f$  are stationary random fields [34].

As  $\vec{E}_f \in \mathcal{H}_\times$  and  $\vec{J}_f \in \mathcal{H}_\bullet$ , equation (2.3) yields the energy (power) [46] constraints  $\langle \vec{J} \cdot \vec{E}_f \rangle = 0$  and  $\langle \vec{E} \cdot \vec{J}_f \rangle = 0$ , respectively, which leads to the following reduced energy representations  $\langle \vec{J} \cdot \vec{E} \rangle = \langle \vec{J} \rangle \cdot \vec{E}_0$  and  $\langle \vec{E} \cdot \vec{J} \rangle = \langle \vec{E} \rangle \cdot \vec{J}_0$ . The effective complex conductivity and resistivity tensors,  $\sigma^*$  and  $\rho^*$ , are defined by

$$\begin{aligned} \langle \vec{J} \rangle &= \sigma^* \vec{E}_0 \\ \langle \vec{E} \rangle &= \rho^* \vec{J}_0. \end{aligned} \quad (2.5)$$

Consequently, we have the following energy representations involving the effective parameters

$$\begin{aligned}\langle \vec{J} \cdot \vec{E} \rangle &= \boldsymbol{\sigma}^* \vec{E}_0 \cdot \vec{E}_0, \\ \langle \vec{E} \cdot \vec{J} \rangle &= \boldsymbol{\rho}^* \vec{J}_0 \cdot \vec{J}_0.\end{aligned}\tag{2.6}$$

We assume that the composite is a locally isotropic random medium so that  $\sigma_{jk}(\vec{x}, \omega) = \sigma(\vec{x}, \omega) \delta_{jk}$  and  $\rho_{jk}(\vec{x}, \omega) = \rho(\vec{x}, \omega) \delta_{jk}$ , where  $\delta_{jk}$  is the Kronecker delta and  $j, k = 1, \dots, d$ . We further assume that the composite is a two-component medium, so that  $\sigma(\vec{x}, \omega)$  takes the *complex* values  $\sigma_1$  and  $\sigma_2$ , and  $\rho(\vec{x}, \omega)$  takes the complex values  $1/\sigma_1$  and  $1/\sigma_2$ , and satisfy [34]

$$\begin{aligned}\sigma(\vec{x}, \omega) &= \sigma_1 \chi_1(\vec{x}, \omega) + \sigma_2 \chi_2(\vec{x}, \omega), \\ \rho(\vec{x}, \omega) &= \sigma_1^{-1} \chi_1(\vec{x}, \omega) + \sigma_2^{-1} \chi_2(\vec{x}, \omega).\end{aligned}\tag{2.7}$$

Here,  $\chi_i(\vec{x}, \omega)$  is the characteristic function of medium  $i = 1, 2$ , which equals one for all  $\omega \in \Omega$  having medium  $i$  at  $\vec{x}$  and zero otherwise, with  $\chi_1 = 1 - \chi_2$ . For simplicity, we focus on one component,  $\sigma_{jk}^* = [\boldsymbol{\sigma}^*]_{jk}$  and  $\rho_{jk}^* = [\boldsymbol{\rho}^*]_{jk}$ , of these symmetric tensors, for some  $j, k = 1, \dots, d$ .

Due to the homogeneity of these functions, e.g.,  $\sigma_{jk}^*(a\sigma_1, a\sigma_2) = a\sigma_{jk}^*(\sigma_1, \sigma_2)$  for any complex number  $a$ , they depend only on the ratio  $h = \sigma_1/\sigma_2$ , and we define the tensor-valued functions  $\mathbf{m}(h) = \boldsymbol{\sigma}^*/\sigma_2$ ,  $\mathbf{w}(z) = \boldsymbol{\sigma}^*/\sigma_1$ ,  $\tilde{\mathbf{m}}(h) = \sigma_1 \boldsymbol{\rho}^*$ , and  $\tilde{\mathbf{w}}(z) = \sigma_2 \boldsymbol{\rho}^*$  with components

$$\begin{aligned}m_{jk}(h) &= \sigma_{jk}^*/\sigma_2, & w_{jk}(z) &= \sigma_{jk}^*/\sigma_1, \\ \tilde{m}_{jk}(h) &= \sigma_1 \rho_{jk}^*, & \tilde{w}_{jk}(z) &= \sigma_2 \rho_{jk}^*,\end{aligned}\tag{2.8}$$

where  $z = 1/h$ . The dimensionless functions  $m_{jk}(h)$  and  $\tilde{m}_{jk}(h)$  are analytic off the negative real axis in the  $h$ -plane, while  $w_{jk}(z)$  and  $\tilde{w}_{jk}(z)$  are analytic off the negative real axis in the  $z$ -plane [34]. Each take the corresponding upper half plane to the upper half plane and are therefore examples of Herglotz functions [22, 34].

A key step in the ACM is obtaining Stieltjes integral representations for  $\boldsymbol{\sigma}^*$  and  $\boldsymbol{\rho}^*$ . These follow from resolvent representations for the electric field  $\vec{E}$  [34] and current density  $\vec{J}$  [60]

$$\begin{aligned}\vec{E} &= s(sI - \Gamma\chi_1)^{-1} \vec{E}_0 = t(tI - \Gamma\chi_2)^{-1} \vec{E}_0, & s \in \mathbb{C} \setminus [0, 1], \\ \vec{J} &= t(tI - \Upsilon\chi_1)^{-1} \vec{J}_0 = s(sI - \Upsilon\chi_2)^{-1} \vec{J}_0, & t \in \mathbb{C} \setminus [0, 1],\end{aligned}\tag{2.9}$$

where  $I$  is the identity operator on  $\mathbb{R}^d$  and we have defined the complex variables  $s = 1/(1-h)$  and  $t = 1/(1-z) = 1-s$ . The operator  $\Gamma = \vec{\nabla}(\Delta^{-1})\vec{\nabla} \cdot$  is based on convolution with the free-space Green's function for the Laplacian  $\Delta = \vec{\nabla} \cdot \vec{\nabla} = \nabla^2$ , and the operator  $\Upsilon = \vec{\nabla} \times (\vec{\nabla} \times \vec{\nabla} \times)^{-1} \vec{\nabla} \times$  involves the vector Laplacian  $\boldsymbol{\Delta} = -\vec{\nabla} \times \vec{\nabla} \times + \vec{\nabla} \vec{\nabla} \cdot$  when  $d=3$  [34, 60]. These (non-random) integro-differential operators and the origin of the resolvent equations in (2.9) are discussed in more detail below.

If the current density  $\vec{J}(\vec{x}, \omega)$  and the electric field  $\vec{E}(\vec{x}, \omega)$  are sufficiently smooth for all  $\vec{x} \in \mathbb{R}^d$  when  $\omega \in \Omega$ , equation (2.9) is obtained as follows. The operator  $\Delta^{-1}$  is well defined in terms of convolution with respect to the free-space Green's function of the Laplacian  $\Delta$  [34, 26]. Similarly, the inverse  $\boldsymbol{\Delta}^{-1}$  of the vector Laplacian  $\boldsymbol{\Delta}$  is defined in terms of component-wise convolution with respect to the free-space Green's function of the Laplacian.

Applying the integro-differential operator  $\vec{\nabla}(\Delta^{-1})$  to the formula  $\vec{\nabla} \cdot \vec{J} = 0$  in equation (2.4) yields  $\Gamma \vec{J} = 0$ , where  $\Gamma = \vec{\nabla}(\Delta^{-1})\vec{\nabla} \cdot$  is an orthogonal projection [34] from  $\mathcal{H}$  onto the Hilbert space  $\mathcal{H}_\times$  of curl-free random fields,  $\Gamma : \mathcal{H} \mapsto \mathcal{H}_\times$ . More specifically, for every sufficiently smooth  $\vec{\zeta} \in \mathcal{H}_\times$  there exists [46] a scalar potential  $\varphi$  which is unique up to a constant such that  $\vec{\zeta} = \vec{\nabla}\varphi$ . Consequently, since  $\Delta = \vec{\nabla} \cdot \vec{\nabla}$ , it is clear that  $\Gamma \vec{\zeta} = \vec{\zeta}$  for all such  $\vec{\zeta} \in \mathcal{H}_\times$ .

For simplicity, we discuss only the analogous properties of divergence free vector fields and the projection operator  $\Upsilon = \vec{\nabla} \times (\vec{\nabla} \times \vec{\nabla} \times)^{-1} \vec{\nabla} \times$ , restricting our attention to  $d=3$  to avoid a more involved discussion regarding differential forms [19]. Applying the integro-differential operator  $-\vec{\nabla} \times (\Delta^{-1})$  to the formula  $\vec{\nabla} \times \vec{E} = 0$  in equation (2.4) yields  $\Upsilon \vec{E} = 0$ . Here,  $\Upsilon = -\vec{\nabla} \times (\Delta^{-1})\vec{\nabla} \times$  is an orthogonal projection from  $\mathcal{H}$  onto the Hilbert space  $\mathcal{H}_\bullet$  of divergence-free random fields,  $\Upsilon : \mathcal{H} \mapsto \mathcal{H}_\bullet$ , of transverse gauge [60]. This can be seen as follows. For every sufficiently smooth  $\vec{\zeta} \in \mathcal{H}_\bullet$  we have the representation  $\vec{\zeta} = \vec{\nabla} \times (\vec{A} + \vec{C})$ , where  $\vec{A}$  is a vector potential associated with  $\vec{\zeta}$  and the arbitrary vector field  $\vec{C}$  satisfies  $\vec{\nabla} \times \vec{C} = 0$  [46]. Without loss of generality, the vector field  $\vec{C}$  can be chosen so that  $\vec{A}$  satisfies  $\vec{\nabla} \cdot \vec{A} = 0$  [46]. Hence,  $\vec{\nabla} \times \vec{\zeta} = \vec{\nabla} \times \vec{\nabla} \times \vec{A} = \vec{\nabla}(\vec{\nabla} \cdot \vec{A}) - \Delta \vec{A} = -\Delta \vec{A}$ . The vector field  $\vec{C}$  chosen in this manner gives the transverse *gauge* of  $\vec{\zeta}$  [46]. Choosing the members of  $\mathcal{H}_\bullet$  to have transverse gauge, the action of  $\vec{\nabla} \times \vec{\nabla} \times$  on  $\mathcal{H}_\bullet$  is given by that of  $-\Delta$ . Therefore, the action of  $\Upsilon$  on  $\mathcal{H}_\bullet$  is given by that of

$$\Upsilon = \vec{\nabla} \times (\vec{\nabla} \times \vec{\nabla} \times)^{-1} \vec{\nabla} \times = -\vec{\nabla} \times (\Delta^{-1}) \vec{\nabla} \times, \quad (2.10)$$

and it is clear from the above discussion that  $\Upsilon \vec{\zeta} = \vec{\zeta}$  for all such  $\vec{\zeta} \in \mathcal{H}_\bullet$ . In general, the differential operators  $\vec{\nabla}$ ,  $\vec{\nabla} \cdot$ , and  $\vec{\nabla} \times$  are interpreted in a weak sense in terms of the operators  $L_i$  in (2.1) [34].

We now derive the resolvent formulas in equation (2.9). Write  $\sigma$  and  $\rho$  in equation (2.7) as  $\sigma = \sigma_2(1 - \chi_1/s) = \sigma_1(1 - \chi_2/t)$  and  $\rho = (1 - \chi_2/s)/\sigma_1 = (1 - \chi_1/t)/\sigma_2$ . Recall that  $\vec{E} = \vec{E}_0 + \vec{E}_f$ , where  $\vec{E}_0$  is a *constant* field and  $\vec{E}_f \in \mathcal{H}_\times$  so that  $\Gamma \vec{E} = \vec{E}_f$ , and similarly  $\Upsilon \vec{J} = \vec{J}_f$ . Consequently, from  $\Gamma \vec{J} = 0$  and  $\Upsilon \vec{E} = 0$  we have the following formulas which are equivalent to that in (2.9)

$$\begin{aligned} \vec{E}_f &= \frac{1}{s} \Gamma \chi_1 \vec{E} = \frac{1}{t} \Gamma \chi_2 \vec{E}, \\ \vec{J}_f &= \frac{1}{s} \Upsilon \chi_2 \vec{J} = \frac{1}{t} \Upsilon \chi_1 \vec{J}. \end{aligned} \quad (2.11)$$

On the Hilbert space  $\mathcal{H}_\times$ , the operators  $\Gamma$  and  $\chi_i$ ,  $i=1,2$ , act as projectors [34]. Therefore  $M_i = \chi_i \Gamma \chi_i$ ,  $i=1,2$ , are compositions of projection operators on  $\mathcal{H}_\times$ , and are consequently positive definite and bounded by 1 in the underlying operator norm [71]. They are self-adjoint with respect to the  $\mathcal{H}$ -inner-product  $\langle \cdot, \cdot \rangle$  [34]. Therefore, on the Hilbert space  $\mathcal{H}_\times$  with weight  $\chi_1$  in the inner-product,  $\langle \cdot, \cdot \rangle_1 = \langle \chi_1 \cdot, \cdot \rangle$  for example,  $\Gamma \chi_1$  is a bounded linear self-adjoint operator with spectrum contained in the interval  $[0, 1]$  [34, 26, 71]. Hence the resolvent operator  $(sI - \Gamma \chi_1)^{-1}$  in (2.9) is also a linear self-adjoint operator with respect to the same inner-product, and is bounded for  $s \in \mathbb{C} \setminus [0, 1]$  [79]. Similarly,  $(tI - \Upsilon \chi_1)^{-1}$  in (2.9) is a linear self-adjoint operator on  $\mathcal{H}_\bullet$  with respect to the inner-product  $\langle \cdot, \cdot \rangle_1$ , and is bounded for  $t \in \mathbb{C} \setminus [0, 1]$ .

To obtain integral representations for  $\sigma^*$  and  $\rho^*$ , it is more convenient to consider the functions  $F_{jk}(s) = \delta_{jk} - m_{jk}(h)$  and  $E_{jk}(s) = \delta_{jk} - \tilde{m}_{jk}(h)$  which are analytic off

$[0,1]$  in the  $s$ -plane, and  $G_{jk}(t) = \delta_{jk} - w_{jk}(z)$  and  $H_{jk}(t) = \delta_{jk} - \tilde{w}_{jk}(z)$  which are analytic off  $[0,1]$  in the  $t$ -plane [34]. For the formulation of the effective parameter problem involving  $\mathcal{H}_\times$  and  $\sigma^*$ , define the coordinate system so that in (2.5) the constant vector  $\vec{E}_0$  is given by  $\vec{E}_0 = E_0 \vec{e}_j$ , where  $\vec{e}_j$  is the standard basis vector on  $\mathbb{R}^d$  in the  $j^{\text{th}}$  direction for some  $j=1, \dots, d$ . In the other formulation involving  $\mathcal{H}_\bullet$  and  $\rho^*$ , define  $\vec{J}_0 = J_0 \vec{e}_j$ . Equations (2.5) and (2.9), and the spectral theorem for bounded linear self-adjoint operators [70, 79] then yield the following Stieltjes integral representations [34, 6, 8, 60] for the effective parameters  $\sigma_{jk}^*$  and  $\rho_{jk}^*$  (see Sections 2.2.3 and A-1.1 for more details)

$$\begin{aligned} m_{jk}(h) &= \delta_{jk} - F_{jk}(s), & F_{jk}(s) &= \langle \chi_1(sI - \Gamma\chi_1)^{-1} \vec{e}_j \cdot \vec{e}_k \rangle = \int_0^1 \frac{d\mu_{jk}(\lambda)}{s - \lambda}, \\ w_{jk}(z) &= \delta_{jk} - G_{jk}(t), & G_{jk}(t) &= \langle \chi_2(tI - \Gamma\chi_2)^{-1} \vec{e}_j \cdot \vec{e}_k \rangle = \int_0^1 \frac{d\alpha_{jk}(\lambda)}{t - \lambda}, \\ \tilde{m}_{jk}(h) &= \delta_{jk} - E_{jk}(s), & E_{jk}(s) &= \langle \chi_2(sI - \Upsilon\chi_2)^{-1} \vec{e}_j \cdot \vec{e}_k \rangle = \int_0^1 \frac{d\eta_{jk}(\lambda)}{s - \lambda}, \\ \tilde{w}_{jk}(z) &= \delta_{jk} - H_{jk}(t), & H_{jk}(t) &= \langle \chi_1(tI - \Upsilon\chi_1)^{-1} \vec{e}_j \cdot \vec{e}_k \rangle = \int_0^1 \frac{d\kappa_{jk}(\lambda)}{t - \lambda}. \end{aligned} \quad (2.12)$$

Equation (2.12) displays Stieltjes integrals involving *spectral measures of random operators*. More specifically,  $d\mu_{jk}(\lambda)$  and  $d\alpha_{jk}(\lambda)$  are spectral measures associated with the random operators  $\chi_1\Gamma\chi_1$  and  $\chi_2\Gamma\chi_2$ , while  $d\eta_{jk}(\lambda)$  and  $d\kappa_{jk}(\lambda)$  are spectral measures associated with the random operators  $\chi_2\Upsilon\chi_2$  and  $\chi_1\Upsilon\chi_1$ , respectively. In particular, there is a one-to-one correspondence between the bounded linear operator  $\chi_1\Gamma\chi_1$  on  $\mathcal{H}_\times$ , for example, and a family of projection operators  $Q(\lambda)$ , parameterized by  $\lambda \in [0,1]$ , which satisfies  $\lim_{\lambda \rightarrow 0} Q(\lambda) = 0$  and  $\lim_{\lambda \rightarrow 1} Q(\lambda) = I$ , where 0 and  $I$  are the null and identity operators on  $\mathcal{H}_\times$ , respectively [79]. The strictly increasing function  $\mu_{jk}(\lambda) = \langle Q(\lambda) \vec{e}_j, \vec{e}_k \rangle_1$  of the spectral variable  $\lambda$  is of bounded variation [79]. The spectral measure  $d\mu_{jk}(\lambda)$  is a *Stieltjes measure* [27] associated with the function  $\mu_{jk}(\lambda)$  [79] (see Section A-1.1 for more details). For notational simplicity, we will often refer to the measure  $\mu_{jk}$ , not to be confused with the function  $\mu_{jk}(\lambda)$ .

By the Stieltjes–Perron inversion theorem [44, 58], the matrix valued function  $\boldsymbol{\mu}(\lambda)$  with components  $\mu_{jk}(\lambda)$ ,  $j, k = 1, \dots, d$ , for example, is given by the weak limit  $\boldsymbol{\mu}(\lambda) = -(1/\pi) \lim_{\varepsilon \downarrow 0} \text{Im}(\mathbf{F}(\lambda + i\varepsilon))$ , i.e.,

$$\int_0^1 \xi(\lambda) d\boldsymbol{\mu}(\lambda) = -\frac{1}{\pi} \lim_{\varepsilon \downarrow 0} \int_0^1 \xi(\lambda) \text{Im}(\mathbf{F}(\lambda + i\varepsilon)) d\lambda, \quad (2.13)$$

for all smooth test functions  $\xi(\lambda)$ , where  $[\mathbf{F}(s)]_{jk} = F_{jk}(s)$  and  $[d\boldsymbol{\mu}(\lambda)]_{jk} = d\mu_{jk}(\lambda)$ . From equation (2.13) and the identities  $m_{jk}(h) = h w_{jk}(z)$  and  $\tilde{m}_{jk}(h) = h \tilde{w}_{jk}(z)$ , which follow from equation (2.8), it has been shown [60] that the functions  $\mu_{jk}(\lambda)$  and  $\alpha_{jk}(\lambda)$ , and the functions  $\eta_{jk}(\lambda)$  and  $\kappa_{jk}(\lambda)$  are related by

$$\begin{aligned} \lambda \alpha_{jk}(\lambda) &= (1 - \lambda) \mu_{jk}(1 - \lambda) + \lambda \varrho(\lambda), & d\varrho(\lambda) &= m_{jk}(0) \delta_0(d\lambda) + w_{jk}(0) (\lambda - 1) \delta_1(d\lambda), \\ \lambda \kappa_{jk}(\lambda) &= (1 - \lambda) \eta_{jk}(1 - \lambda) + \lambda \tilde{\varrho}(\lambda), & d\tilde{\varrho}(\lambda) &= \tilde{m}_{jk}(0) \delta_0(d\lambda) + \tilde{w}_{jk}(0) (\lambda - 1) \delta_1(d\lambda). \end{aligned} \quad (2.14)$$

Here,  $m(0) = m(h)|_{h=0}$  and  $w(0) = w(z)|_{z=0}$ , for example, and  $\delta_a(d\lambda)$  is the delta measure concentrated at  $\lambda = a$ .

Equations (2.12) and (2.14) demonstrate the many symmetries between the functions  $m_{jk}(h)$ ,  $w_{jk}(z)$ ,  $\tilde{m}_{jk}(h)$ , and  $\tilde{w}_{jk}(z)$ , and the respective measures  $\mu_{jk}$ ,  $\alpha_{jk}$ ,  $\eta_{ij}$ , and  $\kappa_{jk}$ . Because of these symmetries, for simplicity, we will focus on  $m_{jk}(h)$  and  $\mu_{jk}$ , and will reintroduce the other functions and measures where appropriate.

A key feature of equations (2.5), (2.8), and (2.12) is that the parameter information in  $h$  and  $E_0$  is *separated* from the geometry of the composite, which is encoded in the spectral measure  $\mu_{jk}$  via its moments  $\mu_{jk}^n$  [34, 11]

$$\mu_{jk}^n = \int_0^1 \lambda^n d\mu_{jk}(\lambda) = \langle \chi_1 [\Gamma \chi_1]^n \vec{e}_j \cdot \vec{e}_k \rangle, \quad n=0,1,2,\dots, \quad (2.15)$$

where the second equality follows from the spectral theorem displayed in equation (A-2) with  $f(\lambda) = \lambda^n$ . Since  $\chi_1$  operates pointwise on  $\mathbb{R}^d$  and the constant vectors  $\vec{e}_j$ ,  $j=1,\dots,d$ , are non-random, we see from equation (2.15) that the mass  $\mu_{jk}^0$  of the measure  $\mu_{jk}$  is given by

$$\mu_{jk}^0 = p_1 \delta_{jk}, \quad (2.16)$$

where  $p_1 = \langle \chi_1 \rangle$  is the volume fraction of material component one. This demonstrates that the diagonal components  $\mu_{kk}$ ,  $k=1,\dots,d$ , of  $\boldsymbol{\mu}$  are *positive measures*, while the off-diagonal components  $\mu_{jk}$ ,  $j \neq k=1,\dots,d$ , have zero mass and are consequently *signed measures* [27, 71]. The positivity of the measure  $\mu_{kk}$  also follows from the fact that  $Q(\lambda)$  is a *self-adjoint projector* on  $\mathcal{H}_\times$  so that  $\langle Q(\lambda) \vec{e}_k \cdot \vec{e}_k \rangle_1 = \langle Q(\lambda) \vec{e}_k \cdot Q(\lambda) \vec{e}_k \rangle_1 = \|Q(\lambda) \vec{e}_k\|_1^2$  is a strictly increasing function of  $\lambda$  [70, 79]. Therefore, the measure of an arbitrary set  $A \subseteq [0,1]$  is positive:

$$\mu_{kk}(A) = \int_A d\mu_{kk}(\lambda) = \int_A d\|Q(\lambda) \vec{e}_k\|_1^2 \geq 0, \quad (2.17)$$

where  $\|\cdot\|_1$  denotes the norm induced by the inner-product  $\langle \cdot, \cdot \rangle_1$ .

The higher order moments  $\mu_{jk}^n$ ,  $n=1,2,3,\dots$ , in principle, may be found using a perturbation expansion of  $F_{jk}(s)$  about a homogeneous medium ( $\sigma_1 = \sigma_2$ ,  $s = \infty$ ) [34]. In particular  $\mu_{jk}^0 = p_1 \delta_{jk}$ , generically, and  $\mu_{jk}^1 = (p_1 p_2 / d) \delta_{jk}$  for a statistically isotropic random medium [34, 32, 11], where  $p_2 = 1 - p_1 = \langle \chi_2 \rangle$  is the volume fraction of material component 2. In the case of a square bond lattice, which is an example of an infinitely interchangeable random medium [11],  $\mu_{kk}^2 = p_1 p_2 (1 + (d-2)p_2) / d^2$  for any dimension  $d$  and  $\mu_{kk}^3 = p_1 p_2 (p_2^2 - p_2 - 1) / 8$  for  $d=2$ . In general, the moments  $\mu_{jk}^n$  depend on the  $(n+1)$ -point correlation functions of the random medium [34, 11].

A principal application of the ACM is to derive *forward bounds* on the diagonal components  $\sigma_{kk}^*$  of the tensor  $\boldsymbol{\sigma}^*$ ,  $k=1,\dots,d$ , given partial information on the microgeometry [7, 55, 34, 8]. This information may be given in terms of the moments  $\mu_{kk}^n$ ,  $n=0,1,2,\dots$ , of the measure  $\mu_{kk}$  [57, 34]. Given this information, the bounds on  $\sigma_{kk}^*$  follow from the special structure of  $F_{kk}(s)$  in (2.12). More specifically, it is a *linear* functional of the *positive* measure  $\mu_{kk}$ . The bounds are obtained by fixing the contrast parameter  $s$ , varying over an admissible set of measures  $\mu_{kk}$  (or geometries) which is determined by the known information regarding the two-component composite. Knowledge of the moments  $\mu_{kk}^n$  for  $n=1,\dots,J$  confines  $\sigma_{kk}^*$  to a region of the complex plane which is bounded by arcs of circles, and the region becomes progressively smaller as more moments are known [57, 28]. When all the moments are known, the measure  $\mu_{kk}$  is uniquely determined [1], hence  $\sigma_{kk}^*$  is explicitly known. The bounding procedure is reviewed in Section 2.3.



We conclude this section with a discussion regarding some consequences of the energy constraints  $\langle \vec{J} \cdot \vec{E}_f \rangle = 0 = \langle \vec{E} \cdot \vec{J}_f \rangle$ , which follow from equation (2.3), and are at the heart of the existence and uniqueness of solutions to the formulas of equation (2.4). We first note that the formulas  $\Gamma \vec{E} = \vec{E}_f$  and  $\Upsilon \vec{J} = \vec{J}_f$  are sufficient conditions for these constraints. The sufficiency of these conditions can be seen by writing  $\sigma = \sigma_2(1 - \chi_1/s)$  and  $\rho = (1 - \chi_1/t)/\sigma_2$  in  $\vec{J} = \sigma \vec{E}$  and  $\vec{E} = \rho \vec{J}$ , respectively, to obtain

$$\langle \vec{J} \cdot \vec{E}_f \rangle = \sigma_2(\langle \vec{E} \cdot \vec{E}_f \rangle - \langle \chi_1 \vec{E} \cdot \vec{E}_f \rangle / s), \quad \langle \vec{E} \cdot \vec{J}_f \rangle = (\langle \vec{J} \cdot \vec{J}_f \rangle - \langle \chi_1 \vec{J} \cdot \vec{J}_f \rangle / t) / \sigma_2, \quad (2.18)$$

for  $s \neq 0$  ( $h \neq +\infty$ ) and  $t \neq 0$  ( $h \neq 0$ ). Now, if we have  $\Gamma \vec{E} = \vec{E}_f$  then  $\vec{\nabla} \cdot \vec{J} = 0$  yields the formula  $\vec{E}_f = \Gamma \chi_1 \vec{E} / s$  of equation (2.11). Therefore, as  $\Gamma$  is a self-adjoint operator on  $\mathcal{H}$  [76, 79, 26], we have

$$\langle \chi_1 \vec{E} \cdot \vec{E}_f \rangle = \langle \chi_1 \vec{E} \cdot \Gamma \vec{E} \rangle = \langle \Gamma \chi_1 \vec{E} \cdot \vec{E} \rangle = s \langle \vec{E}_f \cdot \vec{E} \rangle. \quad (2.19)$$

Consequently, from equation (2.18) we have  $\langle \vec{J} \cdot \vec{E}_f \rangle = 0$  for  $s \neq 0$ . The argument involving the operator  $\Upsilon$  and the vector field  $\vec{J}_f$  is analogous.

We see from equation (2.18) that the energy constraints are equivalent to the following “field representations” for the contrast parameters  $s$  and  $t$

$$\langle \chi_1 \vec{E} \cdot \vec{E}_f \rangle / \langle \vec{E} \cdot \vec{E}_f \rangle = s = 1 - t = 1 - \langle \chi_1 \vec{J} \cdot \vec{J}_f \rangle / \langle \vec{J} \cdot \vec{J}_f \rangle, \quad (2.20)$$

when  $\langle \vec{E} \cdot \vec{E}_f \rangle \neq 0$  (if and only if  $\langle \chi_1 \vec{E} \cdot \vec{E}_f \rangle \neq 0$  when  $s \neq 0$  from (2.19)), for example. Moreover, the energy constraints provide the limiting behavior of the ratio  $\mathcal{R}(h) = \langle \vec{E} \cdot \vec{E}_f \rangle / \langle \chi_1 \vec{E} \cdot \vec{E}_f \rangle = 1/s$ , for example,

$$\lim_{h \rightarrow 0} \mathcal{R}(h) = 1, \quad \lim_{h \rightarrow 1} \mathcal{R}(h) = 0, \quad \lim_{h \rightarrow +\infty} \mathcal{R}(h) = -\infty, \quad (2.21)$$

which is otherwise a very complicated object in the absence of these energy constraints. We also note that equation (2.20) provides a relationship between the members  $\vec{E}_f$  and  $\vec{J}_f$  of the Hilbert spaces  $\mathcal{H}_\times$  and  $\mathcal{H}_\bullet$ , respectively.

The energy constraints also lead to detailed decompositions of the system energy  $\langle \vec{J} \cdot \vec{E} \rangle$  in terms of Herglotz functions involving the measures  $\mu_{jj}$ ,  $\alpha_{jj}$ ,  $\eta_{jj}$ , and  $\kappa_{jj}$  [60, 63]. For example,  $\langle \vec{J} \cdot \vec{E}_f \rangle = 0$ ,  $\vec{E} = \vec{E}_0 + \vec{E}_f$ ,  $\vec{E}_0 = E_0 \vec{e}_j$ ,  $\langle \vec{E}_f \rangle = 0$ , and  $\sigma = \sigma_2(1 - \chi_1/s)$  together imply that  $0 = \langle \sigma \vec{E} \cdot \vec{E}_f \rangle = \langle \sigma_2(1 - \chi_1/s)(\vec{E}_f \cdot \vec{E}_0 + E_f^2) \rangle = \sigma_2 [\langle E_f^2 \rangle - (\langle \chi_1 \vec{E}_f \cdot \vec{E}_0 \rangle + \langle \chi_1 E_f^2 \rangle) / s]$ . Equations (2.9) and (2.12), and the spectral theorem [70] then yield [60]

$$\frac{\langle E_f^2 \rangle}{E_0^2} = \int_0^1 \frac{\lambda d\mu_{jj}(\lambda)}{(s - \lambda)^2} = \int_0^1 \frac{\lambda d\alpha_{jj}(\lambda)}{(t - \lambda)^2}. \quad (2.22)$$

Equation (2.22), in turn, leads to Herglotz representations of all such energy components involving these measures [63]. Analogous energy decompositions involving  $\vec{J}_f$  and the measures  $\eta_{jj}$  and  $\kappa_{jj}$  similarly follow. In [63] this energy decomposition has lead to a physically transparent statistical mechanics model of two-phase dielectric media.

**2.2. Lattice Setting** In this section, we formulate the effective parameter problem for the infinite and finite, two-component bond lattice on  $\mathbb{Z}^d$  (formulations for other lattice topologies are analogous). The infinite bond lattice, reviewed in Section 2.2.1, is a special case of the stationary random medium considered in Section 2.1. In Section 2.2.2, we develop a mathematical framework for the ACM in the finite lattice setting, a key theoretical contribution of this work.

**2.2.1. Infinite Lattice Setting** Consider a two-component bond lattice on all of  $\mathbb{Z}^d$  determined by the probability space  $(\Omega, P)$ , and let  $\sigma(\vec{x}, \omega)$  be the local complex conductivity tensor with components  $\sigma_{jk}(\vec{x}, \omega) = \sigma^j(\vec{x}, \omega) \delta_{jk}$ ,  $j, k = 1, \dots, d$ . Here,  $\sigma^j(\vec{x}, \omega)$  is the conductivity of the bond emanating from  $\vec{x} \in \mathbb{Z}^d$  in the positive  $j^{\text{th}}$  direction for  $\omega \in \Omega$ , which is a stationary random field that takes the *complex* values  $\sigma_1$  and  $\sigma_2$  with probabilities  $p_1$  and  $p_2 = 1 - p_1$ , respectively [29, 11]. The configuration space  $\Omega = \{\sigma_1, \sigma_2\}^{d\mathbb{Z}^d}$  represents the set of all realizations of the random medium and the probability measure  $P$  is compatible with stationarity. Analogous to equation (2.7), the local conductivity  $\sigma^j(\vec{x}, \omega)$  of the two-phase random medium takes the form [29]

$$\sigma^j(\vec{x}, \omega) = \sigma_1 \chi_1^j(\vec{x}, \omega) + \sigma_2 \chi_2^j(\vec{x}, \omega), \quad j = 1, \dots, d. \quad (2.23)$$

Here,  $\chi_i^j(\vec{x}, \omega)$  is the characteristic function of medium  $i = 1, 2$ , which equals one for all realizations  $\omega \in \Omega$  having medium  $i$  in the  $j^{\text{th}}$  positive bond at  $\vec{x}$ , and equals zero otherwise.

In this lattice setting, the differential operators  $\vec{\nabla} \times$  and  $\vec{\nabla} \cdot$  in equation (2.4) are given [29, 11] in terms of forward and backward difference operators  $D_j^+$  and  $D_j^-$ , respectively, where

$$D_j^+ = T_j^+ - I, \quad D_j^- = I - T_j^-, \quad j = 1, \dots, d. \quad (2.24)$$

Here,  $I$  is the identity operator on  $\mathbb{Z}^d$ , and  $T_j^+ = T_{+e_j}$  and  $T_j^- = T_{-e_j}$  are the generators (through composition) of the unitary group  $T_x$  acting on  $L^2(\Omega, P)$  defined by  $(T_x f)(0, \omega) = f(\vec{x}, \omega)$ , for any  $f \in L^2(\Omega, P)$  which is a stationary random field [29]. Define  $\mathcal{H} = \bigotimes_{i=1}^d L^2(\Omega, P)$  and let  $\vec{E}, \vec{J} \in \mathcal{H}$  be the random electric field and current density, respectively, where  $\vec{E}(\vec{x}, \omega) = (E^1(\vec{x}, \omega), \dots, E^d(\vec{x}, \omega))$  and  $E^j(\vec{x}, \omega)$  is the electric field in the bond emanating from  $\vec{x}$  in the positive  $j^{\text{th}}$  direction, and similarly for  $\vec{J}(\vec{x}, \omega)$ .

As in Section 2.1 we write  $\vec{E} = \vec{E}_0 + \vec{E}_f$ , where  $\vec{E}_f$  is the fluctuating field of mean zero about the (constant) average  $\vec{E}_0$ . The variational problem in (2.3) for this lattice setting has a unique solution satisfying Kirchhoff's circuit laws [34, 11]

$$D_i^+ E^j - D_j^+ E^i = 0, \quad \sum_{k=1}^d D_k^- J^k = 0, \quad J^i = \sigma^i E^i, \quad \langle \vec{E} \rangle = \vec{E}_0, \quad (2.25)$$

where  $i, j = 1, \dots, d$  and the components  $E^i(\vec{x}, \omega)$  and  $J^i(\vec{x}, \omega)$  of  $\vec{E}(\vec{x}, \omega)$  and  $\vec{J}(\vec{x}, \omega)$  are stationary random fields. Equation (2.25) is a direct analogue of equation (2.4) when written in component form [34]. The effective complex conductivity tensor  $\sigma^*$  is defined by  $\langle \vec{J} \rangle = \sigma^* \vec{E}_0$ , and has components  $\sigma_{jk}^* = \sigma_2 m_{jk}(h)$ ,  $j, k = 1, \dots, d$ , where  $h = \sigma_1 / \sigma_2$ . The representation formula for  $m_{jk}(h)$  in (2.12) still holds in this infinite lattice setting, with  $\Gamma$  in (2.9) now given by

$$\Gamma = \nabla^+ (\Delta^{-1}) \nabla^-, \quad \nabla^\pm = (D_1^\pm, \dots, D_d^\pm), \quad (2.26)$$

where  $\Delta^{-1}$  is based on discrete convolution with the lattice Green's function for the Laplacian  $\Delta = \nabla^- \nabla^+$  [11]. The formulation of the ACM for the effective resistivity tensor  $\rho^*$  in the infinite lattice setting is analogous to that for  $\sigma^*$  given here. In Section 2.2.2 we discuss in detail the operator  $\Upsilon$  underlying the integral representations for  $\rho^*$  in the lattice setting.

**2.2.2. Finite Lattice Setting** Consider a finite, two-component bond lattice on  $\mathbb{Z}_L^d \subset \mathbb{Z}^d$  determined by the probability space  $(\Omega, P)$ , where

$$\mathbb{Z}_L^d = \{\vec{x} \in \mathbb{Z}^d \mid 1 \leq x_i \leq L, i = 1, \dots, d\}, \quad (2.27)$$

$L \in \mathbb{N}$ ,  $L \geq 2$ , and  $x_i = (\vec{x})_i$  is the  $i^{\text{th}}$  component of the vector  $\vec{x}$ . Let  $\sigma(\vec{x}, \omega)$  be the local complex conductivity tensor with components  $\sigma_{jk}(\vec{x}, \omega) = \sigma^j(\vec{x}, \omega) \delta_{jk}$ ,  $j, k = 1, \dots, d$ , where  $\sigma^j(\vec{x}, \omega)$  is defined in equation (2.23) for  $\vec{x} \in \mathbb{Z}_L^d$  and  $\omega \in \Omega$ . The configuration space  $\Omega = \{\sigma_1, \sigma_2\}^{d\mathbb{Z}_L^d}$  represents the set of all  $2^N$  realizations of the finite random bond lattice, where  $N = dL^d$  and  $P$  is the associated (discrete) probability measure. Define  $\mathcal{H} = \bigotimes_{i=1}^d L^2(\Omega, P)$  and let  $\vec{E}, \vec{J} \in \mathcal{H}$  be the random electric field and current density, respectively, which satisfy Kirchhoff's circuit laws (2.25) with appropriate boundary conditions. Analogous to equation (2.5), the effective complex conductivity tensor  $\sigma^*$  is defined by  $\langle \vec{J} \rangle = \sigma^* \vec{E}_0$ , and has components  $\sigma_{jk}^* = \sigma_2 m_{jk}(h)$ , where  $\vec{E}_0 = \langle \vec{E} \rangle$  and  $\langle \cdot \rangle$  denotes ensemble average over  $\Omega$ . In a similar way we define the functions  $\sigma_{jk}^* = \sigma_1 w_{jk}(z)$  and  $\rho_{jk}^* = \sigma_1 \tilde{m}_{jk}(h) = \sigma_2 \tilde{w}_{jk}(z)$  introduced in Section 2.1.

In this section, we obtain discrete versions of the integral representations for  $m_{jk}(h)$  and  $\tilde{w}_{jk}(z)$  in equation (2.12) for this finite bond lattice setting, involving spectral measures  $\mu_{jk}$  and  $\kappa_{jk}$  associated with real-symmetric random matrices. The formulation involving the functions  $\tilde{m}_{jk}(h)$  and  $w_{jk}(z)$  are analogous. Toward this goal, we define a bijective mapping  $\Theta$  from the  $d$ -dimensional set  $\mathbb{Z}_L^d$  onto the one dimensional set  $\mathbb{N}_L \subset \mathbb{N}$ ,  $\Theta: \mathbb{Z}_L^d \rightarrow \mathbb{N}_L$ , given by

$$\mathbb{N}_L = \{i \in \mathbb{N} \mid i \leq dL^d\}, \quad \Theta(\vec{x}) = x_1 + \sum_{k=2}^d (x_k - 1)L^{k-1}. \quad (2.28)$$

Under the bijection  $\Theta$  the components  $E^j(\vec{x}, \omega)$ ,  $j = 1, \dots, d$ , of the random electric field  $\vec{E}(\vec{x}, \omega) = (E^1(\vec{x}, \omega), \dots, E^d(\vec{x}, \omega))$  are mapped to vector valued functions  $E^j(\vec{x}, \omega) \mapsto \vec{E}^j(\omega) = (E_1^j(\omega), \dots, E_{L^d}^j(\omega))$  so that

$$\Theta(\vec{E}(\vec{x}, \omega)) = (\vec{E}^1(\omega), \dots, \vec{E}^d(\omega)) \in \mathbb{C}^N, \quad (2.29)$$

for each  $\omega \in \Omega$ , and similarly for  $\vec{J}(\vec{x}, \omega)$ . Moreover, the bijection  $\Theta$  maps the standard basis vector  $\vec{e}_1 = (1, 0, \dots, 0) \in \mathbb{Z}^d$ , for example, to the vector  $(\vec{1}, \vec{0}, \dots, \vec{0}) \in \mathbb{Z}^N$ , where  $\vec{1}$  and  $\vec{0}$  are vectors of ones and zeros of length  $L^d$ , respectively, and similarly for the  $\vec{e}_j$  for  $j = 2, \dots, d$ . Therefore, the vectors  $\hat{e}_i$ ,  $i = 1, \dots, d$ , satisfying

$$\hat{e}_i = \Theta(\vec{e}_i)/L^{d/2}, \quad \hat{e}_i \cdot \hat{e}_j = \delta_{ij}, \quad (2.30)$$

serve as the standard basis vectors on  $\mathbb{N}_L$ .

On  $\mathbb{N}_L$  the difference operators  $D_j^\pm$ ,  $j = 1, \dots, d$ , in equation (2.24) are given in terms of finite difference matrices  $D_j$  [23], where the rows of  $D_j$  correspond to the bonds of the lattice, the columns correspond to the nodes, and the numbering of the nodes on  $\mathbb{N}_L$  is determined by the bijection  $\Theta$  in (2.28). In this finite lattice setting, the Laplacian  $\Delta$  and the projection operator  $\Gamma$  in (2.26) are replaced by the real-symmetric matrices  $\Delta = \nabla^T \nabla$  and  $\Gamma = \nabla(\Delta^{-1})\nabla^T$ , respectively, where  $\nabla^T = (D_1^T, \dots, D_d^T)$ . The matrices  $\Delta$  and  $\Gamma$  depend only on the topology and the boundary conditions of the underlying finite bond lattice  $\mathbb{Z}_L^d$ , and  $\Gamma$  is a projection matrix satisfying  $\Gamma^2 = \Gamma$ .

The matrix  $\Gamma$  is invariant under arbitrary permutations in the numbering of the nodes on  $\mathbb{N}_L$ , and is therefore independent of the specific form of the bijective mapping

$\Theta: \mathbb{Z}_L^d \mapsto \mathbb{N}_L$  in equation (2.28). More specifically, let  $\Xi$  be a permutation matrix satisfying  $\Xi^{-1} = \Xi^T$  such that  $\vec{\xi}^T \Xi$  is the vector  $\vec{\xi}^T$  with the entries permuted in an arbitrary manner. Such a permutation in the numbering of the nodes is equivalent to the mapping  $D_j \mapsto D_j \Xi$ ,  $j=1, \dots, d$ . By the properties of transposition and inversion for products of matrices [45], it is easily verified that the matrix  $\Gamma = \nabla(\Delta^{-1})\nabla^T$  is invariant under this mapping. Similarly, permuting the numbering of the bonds is equivalent to the mapping  $D_j \mapsto \Xi D_j$ , and under this mapping  $\Gamma \mapsto \Xi \Gamma \Xi^T$ .

The projection matrix representation of the operator  $\Upsilon$  for the lattice setting is obtained as follows. For simplicity, we restrict our attention to  $d=2,3$ . On  $\mathbb{R}^3$  the curl operation  $\vec{\nabla} \times$  is given by

$$\vec{\nabla} \times \vec{\zeta} = \text{Det} \begin{bmatrix} \vec{e}_1 & \vec{e}_2 & \vec{e}_3 \\ \partial_1 & \partial_2 & \partial_3 \\ \zeta_1 & \zeta_2 & \zeta_3 \end{bmatrix} = C \vec{\zeta}, \quad C = \begin{bmatrix} 0 & -\partial_3 & \partial_2 \\ \partial_3 & 0 & -\partial_1 \\ -\partial_2 & \partial_1 & 0 \end{bmatrix}, \quad (2.31)$$

where  $\vec{\zeta} = \vec{\zeta}(\vec{x})$  for  $\vec{x} \in \mathbb{R}^3$ , we have denoted  $\partial_i$ ,  $i=1,2,3$ , to be partial differentiation in the  $i^{\text{th}}$  direction  $\vec{e}_i$ , and  $C$  is the curl operator  $\vec{\nabla} \times$  in matrix form. One can check directly that  $C^2 = -C^T C = -\Delta + \vec{\nabla} \cdot \vec{\nabla}$ , where  $\Delta$  is the vector Laplacian. The two-dimensional case follows from (2.31) by setting  $\vec{\zeta}(\vec{x}) = [\zeta_1(\vec{x}), \zeta_2(\vec{x}), 0]^T$  with  $\vec{x} = [x_1, x_2, 0]^T$ , yielding

$$\vec{\nabla} \times \vec{\zeta} = (\partial_1 \zeta_2 - \partial_2 \zeta_1) \vec{e}_3 = (\vec{\nabla} \cdot R \vec{\zeta}_2) \vec{e}_3, \quad \vec{\nabla} \cdot = [\partial_1 \ \partial_2], \quad R = \begin{bmatrix} 0 & 1 \\ -1 & 0 \end{bmatrix}, \quad (2.32)$$

where  $R$  is a  $90^\circ$  rotation matrix, we have defined  $\vec{\zeta}_2 = [\zeta_1 \ \zeta_2]^T$ , and the action of  $\vec{\nabla} \cdot R$  on  $\vec{\zeta}_2$  is given by that of the operator  $[-\partial_2 \ \partial_1]$ .

In view of equations (2.25) and (2.31), the matrix representation of the curl operator  $\vec{\nabla} \times$  for the *infinite* lattice setting on  $\mathbb{Z}^3$  is given by  $C$  in (2.31) under the mapping  $\partial_i \mapsto D_i^+$ ,  $i=1,2,3$ , while on  $\mathbb{N}_L$  the curl operator is given by  $C$  in (2.31) under the mapping  $\partial_i \mapsto D_i$ . In two dimensions, pointwise rotations of fields by  $90^\circ$  convert curl free fields to divergence free fields, and vice versa [58]. With this in mind and in view of equation (2.32), in *two-dimensions* it is natural to define the curl operator by  $\vec{\nabla} \times = \vec{\nabla} \cdot R = [-\partial_2 \ \partial_1]$ . Consequently, for the infinite lattice setting on  $\mathbb{Z}^2$  we have  $\vec{\nabla} \times = [-D_2^+ \ D_1^+]$ , while on  $\mathbb{N}_L$  we have

$$\vec{\nabla} \times \vec{\zeta} = C^T \vec{\zeta}, \quad C^T = [-D_2^T \ D_1^T], \quad (2.33)$$

where  $C^T C = \nabla^T \nabla = \Delta$ , the matrix representation of the Laplacian. From the above discussion and in view of equation (2.10), in the lattice setting, it is natural to define the operator  $\Upsilon$  as

$$\Upsilon = \vec{\nabla} \times (\vec{\nabla} \times \vec{\nabla} \times)^{-1} \vec{\nabla} \times = C(C^T C)^{-1} C^T, \quad (2.34)$$

which is clearly a projection operator satisfying  $\Upsilon^2 = \Upsilon$ .

Analogous to the properties of the matrix  $\Gamma$ , in the finite lattice setting the matrix  $\Upsilon$  is invariant under arbitrary permutations in the numbering of the nodes. More specifically, let  $\Xi$  be defined as above and define  $\Xi = \text{diag}(\Xi, \dots, \Xi)$ , so that  $\Xi^{-1} = \Xi^T$ . Such a permutation in the numbering of the nodes is equivalent to the mapping  $C \mapsto C \Xi$ . It is straight forward to verify that  $\Upsilon$  is invariant under this mapping. Similarly, permuting the numbering of the bonds is equivalent to the mapping  $C \mapsto \Xi C$ , and under this mapping  $\Upsilon \mapsto \Xi \Upsilon \Xi^T$ .

We now discuss the matrix representation of the characteristic function  $\chi_1^j(\vec{x}, \omega)$  on  $\mathbb{N}_L$ . By writing the constitutive relation  $J^j(\vec{x}, \omega) = \sigma^j(\vec{x}, \omega) E^j(\vec{x}, \omega)$  displayed in equation (2.25) as  $J^j(\vec{x}, \omega) = \sigma_2(1 - \chi_1^j(\vec{x}, \omega)/s) E^j(\vec{x}, \omega)$ , we see that the characteristic function  $\chi_1^j(\vec{x}, \omega)$  in (2.23) operates on the electric field  $E^j(\vec{x}, \omega)$  in each individual bond  $j = 1, \dots, d$  emanating from  $\vec{x} \in \mathbb{Z}_L^d$ . In view of this and equation (2.29), on  $\mathbb{N}_L$  the characteristic function  $\chi_1^j(\vec{x}, \omega)$  is represented by a block diagonal matrix and

$$\chi_1(\omega) = \text{diag}(\chi_1^1(\omega), \dots, \chi_1^d(\omega)), \quad \chi_2(\omega) = I - \chi_1(\omega), \quad (2.35)$$

where  $\chi_1^j(\omega)$ ,  $j = 1, \dots, d$ , is a *diagonal* matrix of size  $L^d \times L^d$  with zeros and ones distributed according to  $P$  along the main diagonal and  $I$  is the identity matrix on  $\mathbb{R}^N$ . Moreover, the matrix  $\chi_1^j(\omega)$  acts on the vector  $\vec{E}^j(\omega) = \Theta(E^j(\vec{x}, \omega))$  in (2.29) for each  $j = 1, \dots, d$ . Consequently,  $\chi_1(\omega)$  is also a real-symmetric projection matrix of size  $N \times N$ , which determines the geometry and component connectivity of the two-phase random medium. In summary, on  $\mathbb{N}_L$  the operators  $M_1 = \chi_1 \Gamma \chi_1$  and  $K_1 = \chi_1 \Upsilon \chi_1$  are represented by real-symmetric random matrices of size  $N \times N$  [33, 60]. The matrix representations of the operators  $M_2 = \chi_2 \Gamma \chi_2$  and  $K_2 = \chi_2 \Upsilon \chi_2$  are then determined by the relation  $\chi_2(\omega) = I - \chi_1(\omega)$ , where  $I$  is the identity matrix on  $\mathbb{R}^N$ .

The following theorem provides a rigorous mathematical formulation of integral representations for the effective parameters of two-phase random media with finite lattice composite microstructure. The theorem and proof are formulated in terms of the random matrix  $M_1 = \chi_1 \Gamma \chi_1$ . The formulations involving the matrices  $M_2 = \chi_2 \Gamma \chi_2$  and  $K_i = \chi_i \Upsilon \chi_i$ ,  $i = 1, 2$ , are analogous.

**THEOREM 2.1.** *For each  $\omega \in \Omega$ , let  $M_1(\omega) = U(\omega) \Lambda(\omega) U(\omega)$  be the eigenvalue decomposition of the real-symmetric matrix  $M_1(\omega) = \chi_1(\omega) \Gamma \chi_1(\omega)$ . Here, the columns of the matrix  $U(\omega)$  consist of the orthonormal eigenvectors  $\vec{u}_i(\omega)$ ,  $i = 1, \dots, N$ , of  $M_1(\omega)$  and the diagonal matrix  $\Lambda(\omega) = \text{diag}(\lambda_1(\omega), \dots, \lambda_N(\omega))$  involves its eigenvalues  $\lambda_i(\omega)$ . If the electric field  $\vec{E}(\omega)$  satisfies  $\vec{E}(\omega) = \vec{E}_0 + \vec{E}_f(\omega)$ , with  $\vec{E}_0 = \langle \vec{E}(\omega) \rangle$  and  $\Gamma \vec{E}(\omega) = \vec{E}_f(\omega)$ , then the effective complex conductivity tensor  $\sigma^*$  has components  $\sigma_{jk}^* = \sigma_2 m_{jk}(h)$ ,  $j, k = 1, \dots, d$ , which satisfy*

$$m_{jk}(h) = \delta_{jk} - F_{jk}(s), \quad F_{jk}(s) = \int_0^1 \frac{d\mu_{jk}(\lambda)}{s - \lambda}, \quad d\mu_{jk}(\lambda) = \sum_{i=1}^N \langle \delta_{\lambda_i}(d\lambda) \chi_1 Q_i \hat{e}_j \cdot \hat{e}_k \rangle, \quad (2.36)$$

where  $Q_i = \vec{u}_i \vec{u}_i^T$ . Furthermore, the mass  $\mu_{jk}^0$  of the measure  $\mu_{jk}$  satisfies

$$\mu_{jk}^0 = \langle \chi_1 \hat{e}_k \cdot \hat{e}_k \rangle \delta_{jk} = d p_1^k \delta_{jk}. \quad (2.37)$$

Here, we have defined  $p_1^k = \langle N_1^k(\omega) \rangle / N$  to be the average number fraction of type-one bonds in the positive  $k^{\text{th}}$  direction,  $N_1^k(\omega) = \text{Trace}(\chi_1^k(\omega))$  is the total number such bonds for  $\omega \in \Omega$ , and the matrix  $\chi_1^k(\omega)$  is defined in equation (2.35).

Taking  $\vec{E} = \vec{E}_0 + \vec{E}_f$  with the condition  $\Gamma \vec{E} = \vec{E}_f$  as a definition greatly simplifies the proof of Theorem 2.1, by avoiding the formulation and proof of some technical lemmas regarding the commutativity of the matrices  $D_i$ ,  $D_i^T$ ,  $i = 1, \dots, d$ , and  $(\Delta^{-1})$ . To assume the condition  $\Gamma \vec{E} = \vec{E}_f$  is natural, as we showed in equation (2.19) that it is a sufficient condition for the energy constraint  $\langle \vec{J} \cdot \vec{E}_f \rangle = 0$ , which is at the heart of the existence of solutions to equations (2.4) and (2.25) in the infinite, continuum and

lattice settings, respectively. In the finite lattice setting, where  $\Gamma$  and  $\chi_1$  are matrices, this condition leads to equation (2.11) exactly as in Section 2.1.

The proof of Theorem 2.1 is given in Section 2.2.4, after we present a novel formulation of the ACM in Section 2.2.3, which unifies the infinite settings and the finite lattice setting and makes the proof of Theorem 2.1 more transparent. Before we do so, we first introduce an important class of composite microstructures. Namely, the class of finite bond lattices such that  $N_1^k(\omega)$  is a non-random constant  $N_1^k$  for all  $k=1, \dots, d$ , i.e.,  $N_1^k(\omega) = N_1^k$  for all  $\omega \in \Omega$ . Consequently, the number  $N_1(\omega) = \text{Trace}(\chi_1(\omega))$  of ones along the main diagonal of  $\chi_1(\omega)$  satisfies  $N_1(\omega) = N_1$  for all  $\omega \in \Omega$ , with  $N_1 = \sum_k N_1^k$ . Moreover, the number fraction of type-one bonds in the  $k^{\text{th}}$  positive direction is given by  $p_1^k = N_1^k/N$  and the total number fraction of type-one bonds is given by  $p_1 = N_1/N$ , with  $p_1 = \sum_k p_1^k$ .

Given a fixed number fraction  $p_1$  of type-one bonds, one can define a class of highly *anisotropic* composites by fixing  $p_1^k$  close to  $p_1$  for some  $k=1, \dots, d$ , i.e.,  $p_1 - p_1^k \ll 1$ . A class of *locally isotropic* random media is obtained by requiring that every bond emanating from  $\vec{x} \in \mathbb{Z}_L^d$  in the positive direction is of the same type, i.e.,  $\chi_1^j(\omega) = \chi_1^k(\omega)$  for all  $j, k=1, \dots, d$  and  $\omega \in \Omega$ . Hence  $N_1^j = N_1^k$  for all  $j, k=1, \dots, d$ , so that  $N_1^k = N_1/d$  and  $p_1^k = p_1/d$  for all  $k=1, \dots, d$ . In this case, equation (2.37) reduces to

$$\mu_{jk}^0 = p_1 \delta_{jk}, \quad (2.38)$$

which is a direct analogue of equation (2.16). Equation (2.38) also holds for *statistically isotropic* random media, where the total number  $N_1$  of type-one bonds is fixed and randomly distributed in a uniform fashion among the the total number  $N$  of bonds. In other words, the main diagonals of the matrices  $\chi_1(\omega)$ ,  $\omega \in \Omega$ , are random permutations of one another. In this case, the  $N_1^k(\omega)$ ,  $k=1, \dots, d$ , are independent, identically distributed random variables with mean  $\langle N_1^k(\omega) \rangle = p_1 N/d$ .

We note that, by the law of large numbers [25], the formula  $\mu_{jk}^0 = d p_1^k \delta_{jk}$  in equation (2.37) also holds in the infinite lattice setting, where  $p_1^k = \lim_{N \rightarrow \infty} \langle N_1^k(\omega) \rangle / N$  is the volume fraction of type-one bonds in the  $k^{\text{th}}$  direction. Here, the infinite lattice is obtained as the infinite volume limit  $L \rightarrow \infty$  ( $N \rightarrow \infty$ ) of the finite lattice – with  $\mathbb{Z}_L^d$  in (2.27) redefined in a suitable way so that  $\lim_{L \rightarrow \infty} \mathbb{Z}_L^d = \mathbb{Z}^d$ . Consequently, equation (2.38) also holds in the infinite lattice setting for locally and statistically isotropic random media.

**2.2.3. Unifying formulation of the ACM for the finite lattice setting and the infinite settings** When considering the formulation of Stieltjes integral representations for the effective parameters of two-phase random media with finite lattice composite microstructure, there is a fundamental issue with the original formulation of the ACM given in Sections 2.1 and 2.2.1. Namely, the original formulation [34, 10] holds for the *infinite* continuum and lattice settings, but it is incompatible with the *finite* lattice setting of Section 2.2.2. In this section, we address this issue by providing a novel formulation of the ACM, which is equivalent to the original formulation and holds for both the finite lattice setting and the infinite settings.

In the infinite settings, the (infinite-dimensional) operator  $\Gamma\chi_1$  appears in the bilinear functional underlying the Stieltjes integral representation for the effective conductivity tensor  $\sigma^* = \sigma_2 \mathbf{m}(h)$ , displayed in equation (2.12). The underlying Hilbert space is  $\mathcal{H}_\times$ , defined in (2.2), equipped with the  $\mathcal{H}$ -inner-product weighted by the characteristic function  $\chi_1$ , and  $\Gamma\chi_1$  is a self-adjoint operator on  $\mathcal{H}_\times$  with respect to this inner-product. In this abstract (infinite-dimensional) Hilbert space formulation

of the effective parameter problem, the resolvent  $(sI - \Gamma\chi_1)^{-1}$  is also self-adjoint with respect to this inner-product [79].

In contrast, the finite lattice formulation of the effective parameter problem involves a finite dimensional Hilbert space, and the operators  $\Gamma$  and  $\chi_1$  are real-symmetric, non-commutable matrices. In this case, the matrix  $\Gamma\chi_1$  is *not* symmetric, it typically has complex spectrum, and it may not even have a full set of eigenvectors. Consequently, the resolvent  $(sI - \Gamma\chi_1)^{-1}$  of this matrix is not symmetric and, in general, is not defined for all  $s \in \mathbb{C} \setminus [0, 1]$  as required. Therefore, the integral formula of Theorem 2.1 displayed in equation (2.36), which follows from the spectral theorem displayed in equations (A-4) and (??) for the *real-symmetric* matrix  $\chi_1\Gamma\chi_1$ , fails to hold for the matrix  $\Gamma\chi_1$ , in general. Due to this fundamental difference of the finite lattice setting, the mathematical framework must be modified from that of the infinite settings, discussed in Sections 2.1 and 2.2.1.

We now develop a novel formulation of the ACM which holds for both the finite lattice setting and the infinite settings, and yields the integral representations for the effective parameters displayed in equations (2.12) and (2.36). To make the formulation independent of the setting, whether finite or infinite, we make use of generic terms such as symmetric operator, for example, which means real-symmetric matrix in the finite lattice setting and self-adjoint operator in the infinite settings. Essential differences in notation will be explicitly stated.

Recall the definition of the effective conductivity tensor  $\langle \vec{J} \rangle = \langle \sigma \vec{E} \rangle = \sigma^* \langle \vec{E} \rangle$  and that  $\sigma = \sigma_2(1 - \chi_1/s)$  and  $\langle \vec{E} \rangle = \vec{E}_0$ , together yielding

$$\sigma^* \vec{E}_0 = \sigma_2(\vec{E}_0 - \langle \chi_1 \vec{E} \rangle / s). \quad (2.39)$$

Define the coordinate system so that  $\vec{E}_0 = E_0 \vec{e}_j$  for some  $j = 1, \dots, d$  (in the matrix formulation  $\vec{e}_j \mapsto \hat{e}_j$ , where  $\hat{e}_j$  is defined in equation (2.30)). Therefore, taking the dot product of equation (2.39) with the (non-random) basis vector  $\vec{e}_k$  yields

$$\sigma_{jk}^* = \sigma^* \vec{e}_j \cdot \vec{e}_k = \sigma_2 \left( \delta_{jk} - \langle \chi_1 \vec{E} \cdot \vec{e}_k \rangle / (sE_0) \right). \quad (2.40)$$

This demonstrates that the key functional underlying the Stieltjes integral representation for the effective complex conductivity tensor is  $\langle \chi_1 \vec{E} \cdot \vec{e}_k \rangle$ . In fact, in view of equations (2.12) and (2.40), we have that  $F_{jk}(s) = \langle \chi_1 \vec{E} \cdot \vec{e}_k \rangle / (sE_0)$ .

We now derive a resolvent formula for the vector field  $\chi_1 \vec{E}$  involving the symmetric operator  $\chi_1 \Gamma \chi_1$ . With use of the identity  $\vec{E} = \vec{E}_0 + \vec{E}_f$  we rewrite the first formula of equation (2.11) as

$$(sI - \Gamma\chi_1)\vec{E} = s\vec{E}_0, \quad (2.41)$$

where  $I$  is the identity operator on the underlying vector space ( $\mathbb{R}^d$  for the infinite settings and  $\mathbb{R}^N$  for the finite lattice setting). It is now clear that the formula for  $m_{jk}(h) = \sigma_{jk}^* / \sigma_2$  displayed in (2.12) follows by writing the formula in equation (2.41) as  $\vec{E} = s(sI - \Gamma\chi_1)^{-1} \vec{E}_0$  with  $\vec{E}_0 = E_0 \vec{e}_j$ , and substituting this into (2.40). We wish to derive an analogous formula for  $m_{jk}(h)$  involving the symmetric operator  $\chi_1 \Gamma \chi_1$ . In order to introduce this operator and to isolate  $\chi_1 \vec{E}$  in equation (2.41), we premultiply this formula by the *projection* operator  $\chi_1$ , yielding

$$(sI - \chi_1 \Gamma \chi_1)[\chi_1 \vec{E}] = s\chi_1 \vec{E}_0. \quad (2.42)$$

Equation (2.42) is equivalent to the following resolvent formula for  $\chi_1 \vec{E}$

$$\chi_1 \vec{E} = s(sI - \chi_1 \Gamma \chi_1)^{-1} \chi_1 \vec{E}_0, \quad (2.43)$$

which is analogous to that of equation (2.9) for the electric field  $\vec{E}$ . Inserting the formula for  $\chi_1 \vec{E}$  in (2.43), with  $\vec{E}_0 = E_0 \vec{e}_j$ , into equation (2.40) and using the spectral theorem for the symmetric operator  $\chi_1 \Gamma \chi_1$  displayed in equations (A-2), (A-4), and (??), yields the following Stieltjes integral representation for  $m_{jk}(h) = \sigma_{jk}^* / \sigma_2$

$$m_{jk}(h) = \delta_{jk} - F_{jk}(s), \quad F_{jk}(s) = \langle (sI - \chi_1 \Gamma \chi_1)^{-1} \chi_1 \vec{e}_j \cdot \vec{e}_k \rangle = \int_0^1 \frac{d\mu_{jk}(\lambda)}{s - \lambda}. \quad (2.44)$$

This demonstrates that, as in the formulation of the ACM given in Section 2.1, the natural Hilbert space underlying the integral representation in equation (2.44) is  $\mathcal{H}_\times$  equipped with the  $\mathcal{H}$ -inner-product weighted by  $\chi_1$ . However, in Section 2.1 the weighting of the inner-product is defined by premultiplication of  $\chi_1$ , so that  $\langle f(\Gamma \chi_1) \vec{e}_j, \vec{e}_k \rangle_1 = \langle \chi_1 f(\Gamma \chi_1) \vec{e}_j, \vec{e}_k \rangle$ , for all complex valued functions  $f \in L^2(\mu_{jk})$ . Here, the weighting of the inner-product is defined by post multiplication of  $\chi_1$ , so that the inner-product  $\langle \cdot, \cdot \rangle_1$  is instead defined by  $\langle f(\chi_1 \Gamma \chi_1) \vec{e}_j, \vec{e}_k \rangle_1 = \langle f(\chi_1 \Gamma \chi_1) \chi_1 \vec{e}_j, \vec{e}_k \rangle$ , for all  $f \in L^2(\nu_{jk})$ . In the infinite, continuum and lattice settings, the two inner-product definitions are equivalent, as  $\chi_1$  acts *pointwise* on the underlying vector space ( $\mathbb{R}^d$  in the continuous setting and  $\mathbb{Z}^d$  in the lattice setting). However, in the finite lattice setting where  $\chi_1$  is represented as a matrix, the two inner-product definitions are no longer equivalent, for all such functions  $f$ .

We now argue that the formula for  $m_{jk}(h)$  in equation (2.44) is equivalent to that of equation (2.12) for the infinite, continuum and lattice settings. From equation (2.12) write  $F_{jk}(s; \mu_{jk}) = \langle \chi_1 (sI - \Gamma \chi_1)^{-1} \vec{e}_j \cdot \vec{e}_k \rangle$  and from equation (2.44) write  $\tilde{F}_{jk}(s; \nu_{jk}) = \langle (sI - \chi_1 \Gamma \chi_1)^{-1} \chi_1 \vec{e}_j \cdot \vec{e}_k \rangle$ . We will argue that  $\mu_{jk} \equiv \nu_{jk}$  so that  $F_{jk}(s; \mu_{jk}) \equiv \tilde{F}_{jk}(s; \nu_{jk})$ . From the spectral theorem, we have that the moments  $\mu_{jk}^n$  and  $\nu_{jk}^n$ ,  $n = 0, 1, 2, \dots$ , of the measures  $\mu_{jk}$  and  $\nu_{jk}$  satisfy

$$\mu_{jk}^n = \int_0^1 \lambda^n d\mu_{jk}(\lambda) = \langle \chi_1 [\Gamma \chi_1]^n \vec{e}_j \cdot \vec{e}_k \rangle, \quad \nu_{jk}^n = \int_0^1 \lambda^n d\nu_{jk}(\lambda) = \langle [\chi_1 \Gamma \chi_1]^n \chi_1 \vec{e}_j \cdot \vec{e}_k \rangle. \quad (2.45)$$

However, since  $\chi_1$  is a projection operator, we have that  $\chi_1 = \chi_1^m$  on  $\mathcal{H}_\times$  for all  $m \in \mathbb{N}$ , hence  $\chi_1 [\Gamma \chi_1]^n = [\chi_1 \Gamma \chi_1]^n \chi_1$  on  $\mathcal{H}_\times$  for all  $n = 0, 1, 2, \dots$ . This and equation (2.45) imply that  $\mu_{jk}^n \equiv \nu_{jk}^n$  for all  $n = 0, 1, 2, \dots$ . Since the Hausdorff moment problem is determined [74], i.e., knowledge of all the moments uniquely determines the measure, we have that  $\mu_{jk} \equiv \nu_{jk}$ . This, in turn, implies that  $F_{jk}(s; \mu_{jk}) \equiv \tilde{F}_{jk}(s; \nu_{jk})$ , which is what we set out to establish.

**2.2.4. Proof of Theorem 2.1** In this section, we prove the various assertions of Theorem 2.1, which was stated in Section 2.2.2. In particular, we prove that the functional  $F_{jk}(s) = \langle (sI - \chi_1 \Gamma \chi_1)^{-1} \chi_1 \hat{e}_j \cdot \hat{e}_k \rangle$  in (2.44) (with  $\vec{e}_j \mapsto \hat{e}_j$ ) has the integral representation displayed in equation (2.36), involving the spectral measure  $\mu_{jk}$  of the real-symmetric matrix  $\chi_1 \Gamma \chi_1$ , with mass  $\mu_{jk}^0$  given by that in (2.37). We also provide a projection method for the numerically efficient, rigorous computation of  $\mu_{jk}$ . This projection method is summarized by equations (2.56)–(2.58) below.

Toward this goal, for each  $\omega \in \Omega$ , define the sets  $\mathbb{N}_L^1(\omega)$  and  $\mathbb{N}_L^0(\omega)$  by

$$\mathbb{N}_L^1(\omega) = \{i \in \mathbb{N}_L \mid [\chi_1(\omega)]_{ii} = 1\}, \quad \mathbb{N}_L^0(\omega) = \mathbb{N}_L \setminus \mathbb{N}_L^1(\omega). \quad (2.46)$$



Also, define elementary permutation matrices [23]  $\Pi_{\ell,m}(\omega)$ ,  $\ell, m = 1, \dots, N$ ,  $N = dL^d$ , which satisfy  $\Pi_{\ell,m} = \Pi_{\ell,m}^{-1} = \Pi_{\ell,m}^T$  and  $\Pi_{\ell,m}\vec{\xi}$  is the vector  $\vec{\xi}$  with the  $\ell^{\text{th}}$  and  $m^{\text{th}}$  entries interchanged.

Since  $\chi_1(\omega)$  is a diagonal matrix with  $N_1(\omega)$  ones and  $N_0(\omega) = N - N_1(\omega)$  zeros along its main diagonal, it is clear that there exists a permutation matrix  $\Pi(\omega)$  which is a composition of elementary permutation matrices such that

$$\Pi\chi_1\Pi^T = \begin{bmatrix} 0_{00} & 0_{01} \\ 0_{10} & I_1 \end{bmatrix}, \quad \Pi = \prod_{\ell,m \in \mathbb{N}_L} \Pi_{\ell,m}, \quad (2.47)$$

where  $\ell \in \mathbb{N}_L^1$ ,  $m \in \mathbb{N}_L^0$ ,  $I_1$  is the identity matrix of size  $N_1 \times N_1$ , and  $0_{ab}$  is a matrix of zeros of size  $N_a \times N_b$ , for  $a, b = 0, 1$ . Therefore, since  $\Pi^T = \Pi^{-1}$  we have

$$\begin{aligned} \chi_1\Gamma\chi_1 &= \Pi^T \begin{bmatrix} 0_{00} & 0_{01} \\ 0_{10} & I_1 \end{bmatrix} \Gamma_\Pi \begin{bmatrix} 0_{00} & 0_{01} \\ 0_{10} & I_1 \end{bmatrix} \Pi = \Pi^T \begin{bmatrix} 0_{00} & 0_{01} \\ 0_{10} & \Gamma_1 \end{bmatrix} \Pi = \Pi^T \begin{bmatrix} 0_{00} & 0_{01} \\ 0_{10} & U_1\Lambda_1U_1^T \end{bmatrix} \Pi \\ &= \Pi^T \begin{bmatrix} I_0 & 0_{01} \\ 0_{10} & U_1 \end{bmatrix} \begin{bmatrix} 0_{00} & 0_{01} \\ 0_{10} & \Lambda_1 \end{bmatrix} \begin{bmatrix} I_0 & 0_{01} \\ 0_{10} & U_1^T \end{bmatrix} \Pi, \end{aligned} \quad (2.48)$$

where  $I_0$  is the identity matrix of size  $N_0 \times N_0$ . Here, we have defined the real-symmetric matrix  $\Gamma_\Pi = \Pi\Gamma\Pi^T$ ,  $\Gamma_1$  is its lower right principal sub-matrix of size  $N_1 \times N_1$ , and  $\Gamma_1 = U_1\Lambda_1U_1^T$  is the eigenvalue decomposition of  $\Gamma_1$ . As  $\Gamma_1$  is a real-symmetric matrix,  $U_1$  is an orthogonal matrix [45]. Also, since  $\Gamma_\Pi = \Pi\Gamma\Pi^T$  is a similarity transformation of a projection matrix and  $\Pi\chi_1\Pi^T$  is a projection matrix,  $\Lambda_1$  is a diagonal matrix with entries  $\lambda_i^1 \in [0, 1]$ ,  $i = 1, \dots, N_1$ , along its diagonal [45, 23].

Consequently, equation (2.48) implies that the eigenvalue decomposition of the matrix  $\chi_1\Gamma\chi_1$  is given by

$$\chi_1\Gamma\chi_1 = U\Lambda U^T, \quad U = \Pi^T \begin{bmatrix} I_0 & 0_{01} \\ 0_{10} & U_1 \end{bmatrix}, \quad \Lambda = \begin{bmatrix} 0_{00} & 0_{01} \\ 0_{10} & \Lambda_1 \end{bmatrix}. \quad (2.49)$$

Here,  $U$  is an orthogonal matrix satisfying  $U^TU = UU^T = I$ ,  $I$  is the identity matrix on  $\mathbb{R}^N$ , and  $\Lambda$  is a diagonal matrix with entries  $\lambda_i \in [0, 1]$ ,  $i = 1, \dots, N$ , along its diagonal.

The eigenvalue decomposition of the matrix  $\chi_1\Gamma\chi_1$  displayed in equation (2.49) demonstrates that its resolvent  $(sI - \chi_1\Gamma\chi_1)^{-1}$  is well defined for all  $s \in \mathbb{C} \setminus [0, 1]$ . In particular, by the orthogonality of the matrix  $U$ , it has the following useful representation  $(sI - \chi_1\Gamma\chi_1)^{-1} = U(sI - \Lambda)^{-1}U^T$ , where  $(sI - \Lambda)^{-1}$  is a diagonal matrix with entries  $1/(s - \lambda_i)$  along its diagonal. This, in turn, implies that the functional  $F_{jk}(s) = \langle (sI - \chi_1\Gamma\chi_1)^{-1} \chi_1 \hat{e}_j \cdot \hat{e}_k \rangle$  displayed in equation (2.44) (with  $\vec{e}_j \mapsto \hat{e}_j$ ) can be written as

$$F_{jk}(s) = \langle (sI - \Lambda)^{-1} [\chi_1 U]^T \hat{e}_j \cdot U^T \hat{e}_k \rangle. \quad (2.50)$$

As  $\Pi^T = \Pi^{-1}$ , equations (2.47) and (2.49) imply that

$$\chi_1 U = \Pi^T \begin{bmatrix} 0_{00} & 0_{01} \\ 0_{10} & U_1 \end{bmatrix}, \quad \implies \quad \chi_1 \vec{u}_i = \begin{cases} 0, & \text{for } i = 1, \dots, N_0 \\ \vec{u}_i & \text{otherwise} \end{cases}. \quad (2.51)$$

which, in turn, implies that  $[\chi_1 U]^T \hat{e}_j \cdot U^T \hat{e}_k = [\chi_1 U]^T \hat{e}_j \cdot [\chi_1 U]^T \hat{e}_k$ .

We are now ready to provide the integral representation displayed in (2.36) for the functional  $F_{jk}(s)$  in equation (2.50). Denote by  $Q_i = \vec{u}_i \vec{u}_i^T$ ,  $i = 1, \dots, N$ , the mutually

orthogonal projection matrices,  $Q_\ell Q_m = Q_\ell \delta_{\ell m}$ , onto the eigen-spaces spanned by the orthonormal eigenvectors  $\vec{u}_i$ . Equation (2.51) implies that  $\chi_1 Q_i = Q_i \chi_1 = \chi_1 Q_i \chi_1$ , as  $\chi_1 Q_i = 0$  for  $i = 1, \dots, N_0$  and  $\chi_1 Q_i = Q_i$  otherwise. This allows us to write the quadratic form  $[\chi_1 U]^T \hat{e}_j \cdot [\chi_1 U]^T \hat{e}_k$  as

$$[\chi_1 U]^T \hat{e}_j \cdot [\chi_1 U]^T \hat{e}_k = \sum_{i=1}^N (\chi_1 \vec{u}_i \cdot \hat{e}_j) (\chi_1 \vec{u}_i \cdot \hat{e}_k) = \sum_{i=1}^N \chi_1 Q_i \chi_1 \hat{e}_j \cdot \hat{e}_k = \sum_{i=1}^N \chi_1 Q_i \hat{e}_j \cdot \hat{e}_k. \quad (2.52)$$

This, the property  $[\chi_1 U]^T \hat{e}_j \cdot U^T \hat{e}_k = [\chi_1 U]^T \hat{e}_j \cdot [\chi_1 U]^T \hat{e}_k$ , and equation (2.50) yield

$$F_{jk}(s) = \int_0^1 \frac{d\mu_{jk}(\lambda)}{s - \lambda}, \quad d\mu_{jk}(\lambda) = \sum_{i=1}^N \langle \delta_{\lambda_i}(\mathrm{d}\lambda) \chi_1 Q_i \hat{e}_j \cdot \hat{e}_k \rangle. \quad (2.53)$$

From equation (A-3) we have  $\sum_i Q_i = I$ , which implies that the mass  $\mu_{jk}^0$  of the measure  $\mu_{jk}$  is given by

$$\mu_{jk}^0 = \int_0^1 d\mu_{jk}(\lambda) = \int_0^1 \sum_{i=1}^N \langle \delta_{\lambda_i}(\mathrm{d}\lambda) \chi_1 Q_i \hat{e}_j \cdot \hat{e}_k \rangle = \langle \chi_1 \hat{e}_j \cdot \hat{e}_k \rangle = \langle \chi_1 \hat{e}_k \cdot \hat{e}_k \rangle \delta_{jk}, \quad (2.54)$$

as  $\chi_1$  is a diagonal matrix and the underlying probability space is finite. Therefore, as in the continuum setting, the diagonal components  $\mu_{kk}$  of the matrix valued measure  $\boldsymbol{\mu}$  are positive measures with mass  $\langle \chi_1 \hat{e}_k \cdot \hat{e}_k \rangle = \langle \chi_1 \hat{e}_k \cdot \chi_1 \hat{e}_k \rangle = \langle |\chi_1 \hat{e}_k|^2 \rangle \geq 0$ , as  $\chi_1$  is a symmetric projection matrix, while the off-diagonal components  $\mu_{jk}$ , for  $j \neq k$ , have zero mass and are consequently signed measures.

Using equation (2.35) we may write  $\mu_{jk}^0$  in equation (2.54) in a more suggestive form. Recall that  $\hat{e}_1 = (\vec{1}, \vec{0}, \dots, \vec{0})/L^{d/2}$ , where  $\vec{1}$  and  $\vec{0}$  are vectors of ones and zeros of length  $L^d$ , respectively, and similarly for the  $\vec{e}_j$  for  $j = 2, \dots, d$ . Since  $\chi_1$  is a symmetric projection matrix, equations (2.35) and (2.54) imply that

$$\mu_{jk}^0 = \langle \chi_1 \hat{e}_k \cdot \chi_1 \hat{e}_k \rangle \delta_{jk} = \frac{1}{L^d} \langle \chi_1^k \vec{1} \cdot \chi_1^k \vec{1} \rangle \delta_{jk} = \frac{1}{L^d} \langle \text{Trace}(\chi_1^k) \rangle \delta_{jk} = d \frac{\langle N_1^k(\omega) \rangle}{N} \delta_{jk}, \quad (2.55)$$

where  $N_1^k(\omega) = \text{Trace}(\chi_1^k(\omega))$  is the total number of type-one bonds in the positive  $k^{\text{th}}$  direction for  $\omega \in \Omega$  and  $N = dL^d$ . This proves equation (2.37) and concludes our proof of Theorem 2.1  $\square$ .

We conclude this section with the formulation of a projection method for numerically efficient, rigorous computation of spectral measures and effective parameters for composite media with finite lattice microstructure. Note that the sum in equation (2.53) runs only over the index set  $i = N_0 + 1, \dots, N$ , as equation (2.51) implies that the masses  $\chi_1 Q_i \hat{e}_j \cdot \hat{e}_k$  of the measure  $\mu_{jk}$  are zero for  $i = 1, \dots, N_0$ . Let  $\vec{u}_m^1$  and  $\lambda_m^1$ ,  $m = 1, \dots, N_1$ , denote the eigenvalues and eigenvectors of the  $N_1 \times N_1$  matrix  $\Gamma_1 = U_1 \Lambda_1 U_1^T$ , defined in equation (2.48). Now, write

$$\Pi \hat{e}_j = \begin{bmatrix} \hat{e}_j^{\pi_0} \\ \hat{e}_j^{\pi_1} \end{bmatrix}, \quad (2.56)$$

where  $\hat{e}_j^{\pi_0} \in \mathbb{R}^{N_0}$  and  $\hat{e}_j^{\pi_1} \in \mathbb{R}^{N_1}$ . Therefore, writing the matrix  $\chi_1 U$  in equation (2.51) in block diagonal form,  $\chi_1 U = \Pi^T \text{diag}(0_{00}, U_1)$ , we have that

$$[\chi_1 U]^T \hat{e}_j \cdot [\chi_1 U]^T \hat{e}_k = [\text{diag}(0_{00}, U_1^T) \Pi \hat{e}_j] \cdot [\text{diag}(0_{0,0}, U_1^T) \Pi \hat{e}_k] = [U_1^T \hat{e}_j^{\pi_1}] \cdot [U_1^T \hat{e}_k^{\pi_1}]. \quad (2.57)$$

This, the property  $[\chi_1 U]^T \hat{e}_j \cdot U^T \hat{e}_k = [\chi_1 U]^T \hat{e}_j \cdot [\chi_1 U]^T \hat{e}_k$ , and equation (2.50) yield

$$F_{jk}(s) = \langle (sI_1 - \Lambda_1)^{-1} [U_1^T \hat{e}_j^{\pi_1}] \cdot [U_1^T \hat{e}_k^{\pi_1}] \rangle = \left\langle \sum_{m=1}^{N_1} \frac{(\vec{u}_m^1 \cdot \hat{e}_j^{\pi_1})(\vec{u}_m^1 \cdot \hat{e}_k^{\pi_1})}{s - \lambda_m^1} \right\rangle. \quad (2.58)$$

Equation (2.58) demonstrates that only the spectral information of the matrices  $U_1$  and  $\Lambda_1$  appear in the functional representation for  $F_{jk}(s)$  in (2.50) and its integral representation in (2.36). From a computational standpoint, this means that only the eigenvalues and eigenvectors of the  $N_1 \times N_1$  matrix  $\Gamma_1$  need to be computed in order to compute the spectral measures underlying the integral representations of the effective parameters for finite lattice systems. This is extremely cost effective for large dilute systems, where  $N \gg 1$  and  $N_1 \ll N$ , as the numerical cost of finding all the eigenvalues and eigenvectors of a symmetric  $N \times N$  matrix is  $O(N^3)$  [23].

**2.3. Bounding Procedure** In this section, we review a procedure which yields rigorous bounds for the effective transport coefficients of composite media [34, 28]. The bounding procedure associated with the functions  $F_{kk}(s)$  and  $E_{kk}(s)$ , defined in equation (2.12), for example, fixes the contrast parameter  $s$  and varies over admissible sets of measures  $\mu_{kk}$  and  $\eta_{kk}$ , subject to known information regarding the composite. This information is given in terms of the moments  $\mu_{kk}^n$  and  $\eta_{kk}^n$ ,  $n=0,1,2,\dots$ , of these measures. Knowledge of these moments for  $n=1,\dots,J$  confines the value of the effective complex conductivity  $\sigma_{kk}^*$  to a region of the complex plane which is bounded by arcs of circles, and the region becomes progressively smaller as more moments are known [57, 28]. Since the bounding procedure associated with the functions  $G_{kk}(t)$  and  $H_{kk}(t)$  in (2.12) is analogous, we will focus on that involving  $F_{kk}(s)$  and  $E_{kk}(s)$ .

The bounds for  $\sigma_{kk}^*$  and  $\rho_{kk}^*$  follow from three important properties of the functions  $F_{kk}(s)$  and  $E_{kk}(s)$ . First, their integral representations, displayed in equations (2.12) and (2.36), *separate* parameter information in  $s$  and  $E_0$  from the geometry of the composite, which is encoded in the underlying spectral measures  $\mu_{kk}$  and  $\eta_{kk}$  via their moments  $\mu_{kk}^n$  and  $\eta_{kk}^n$ ,  $n=0,1,2,\dots$  [11, 34]. Second, these integral representations are *linear* functionals of the spectral measures. Finally,  $\mu_{kk}$  and  $\eta_{kk}$  are *positive* measures, in contrast to  $\mu_{jk}$  and  $\eta_{jk}$  for  $j \neq k$ . In this section, we review how these three properties yield rigorous bounds for the diagonal components of the effective parameters  $\sigma_{kk}^*$  and  $\rho_{kk}^*$  [34, 28].

We start our discussion with the masses  $\mu_{kk}^0$  and  $\eta_{kk}^0$  of the measures  $\mu_{kk}$  and  $\eta_{kk}$  for the continuum and lattice settings. By equation (2.16) and the symmetries between the functions  $F_{kk}(s)$  and  $E_{kk}(s)$  displayed in equation (2.12), in the continuum setting, the masses  $\mu_{kk}^0$  and  $\eta_{kk}^0$  of the measures  $\mu_{kk}$  and  $\eta_{kk}$  are generically given by  $\mu_{kk}^0 = p_1$  and  $\eta_{kk}^0 = p_2$ , so that

$$\mu_{kk}^0 + \eta_{kk}^0 = 1, \quad k=1,\dots,d. \quad (2.59)$$

By equation (2.37), in the finite lattice setting, we have  $\mu_{kk}^0 = dp_1^k$  generically. The masses  $\mu_{kk}^0$  and  $\eta_{kk}^0$  of the measures  $\mu_{kk}$  and  $\eta_{kk}$  are related in this finite lattice setting as follows. From equation (2.35) we have that  $\chi_1^k(\omega) + \chi_2^k(\omega) = I_{L^d}$  for all  $k=1,\dots,d$  and  $\omega \in \Omega$ , where  $I_{L^d}$  is the identity matrix of size  $L^d \times L^d$ . Consequently, by the linearity of the trace operation, we have that  $\text{Trace}(\chi_1^k(\omega)) + \text{Trace}(\chi_2^k(\omega)) = \text{Trace}(I_{L^d})$ , thus  $N_1^k(\omega) + N_2^k(\omega) = L^d = N/d$ . Averaging this formula over  $\Omega$  and rearranging yields equation (2.59), where  $\eta_{kk}^0 = dp_2^k$  and  $p_2^k = \langle N_2^k(\omega) \rangle / N$  is the average number fraction of type-two bonds in the positive  $k^{\text{th}}$  direction. For isotropic random media with finite lattice composite microstructure, we have from (2.38) that

$\mu_{kk}^0 = p_1$  and  $\eta_{kk}^0 = p_2$ . By the discussion in the paragraph following equation (2.38), the formulas  $\mu_{kk}^0 = dp_1^k$  and  $\eta_{kk}^0 = dp_2^k$  also hold for the infinite lattice setting with  $p_i^k = \lim_{N \rightarrow \infty} \langle N_i(\omega) \rangle / N$ ,  $i = 1, 2$ , and are given by  $\mu_{kk}^0 = p_1$  and  $\eta_{kk}^0 = p_2$  for isotropic random media.

For simplicity, we will focus on one diagonal component  $\sigma_{kk}^*$  and  $\rho_{kk}^*$  of the effective conductivity and resistivity tensors  $\sigma^*$  and  $\rho^*$ , for some  $k = 1, \dots, d$ , and set  $\sigma^* = \sigma_{kk}^*$ ,  $F(s) = F_{kk}(s)$ ,  $m(h) = m_{kk}(h)$ ,  $\mu = \mu_{kk}$ ,  $E(s) = E_{kk}(s)$ ,  $\tilde{m}(h) = \tilde{m}_{kk}(h)$ , and  $\eta = \eta_{kk}$ . Here,  $F(s) = 1 - m(h)$  and  $E(s) = 1 - \tilde{m}(h)$ . We will also exploit the symmetries between  $F(s)$  and  $E(s)$  in equation (2.12) and initially focus on the function  $F(s)$  and the measure  $\mu$ , referring to the function  $E(s)$  and the measure  $\eta$  where appropriate.

Bounds for  $\sigma^*$  are obtained as follows, while those for  $\rho^*$  are obtained analogously. The support of the measure  $\mu$  is contained in the interval  $[0, 1]$  and its mass is given by  $\mu^0 = p_1$ , where  $0 \leq p_1 \leq 1$ . Consider the set  $\mathcal{M}$  of positive Borel measures on  $[0, 1]$  with mass  $\leq 1$ . By equation (2.12), for fixed  $s \in \mathbb{C} \setminus [0, 1]$ ,  $F(s)$  is a linear functional of the measure  $\mu$ ,  $F: \mathcal{M} \mapsto \mathbb{C}$ , and we write  $F(s) = F(s, \mu)$  and  $m(h) = m(h, \mu)$ . Suppose that we know the moments  $\mu^n$  of the measure  $\mu$  for  $n = 0, \dots, J$ . Define the set  $\mathcal{M}_J^\mu \subset \mathcal{M}$  of measures by

$$\mathcal{M}_J^\mu = \left\{ \nu \in \mathcal{M} \mid \int_0^1 \lambda^n d\nu(\lambda) = \mu^n, \ n = 0, \dots, J \right\}. \quad (2.60)$$

The set  $A_J^\mu \subset \mathbb{C}$  that represents the possible values of  $m(h, \mu) = 1 - F(s, \mu)$  which is compatible with the known information about the random medium is given by

$$A_J^\mu = \{ m(h, \mu) \in \mathbb{C} \mid h \notin (-\infty, 0], \ \mu \in \mathcal{M}_J^\mu \}. \quad (2.61)$$

The set of measures  $\mathcal{M}_J^\mu$  is a compact, convex subset of  $\mathcal{M}$  with the topology of weak convergence [34]. Since the mapping  $F(s, \mu)$  in (2.12) is linear in  $\mu$  it follows that  $A_J^\mu$  is a compact convex subset of the complex plane  $\mathbb{C}$ . The extreme points of  $\mathcal{M}_0^\mu$  are the one point measures  $a\delta_b$ ,  $0 \leq a, b \leq 1$  [24], while the extreme points of  $\mathcal{M}_J^\mu$  for  $J > 0$  are weak limits of convex combinations of measures of the form [48, 34]

$$d\mu_J(\lambda) = \sum_{i=1}^{J+1} a_i \delta_{b_i}(d\lambda), \quad a_i \geq 0, \quad 0 \leq b_1 < \dots < b_{J+1} < 1, \quad \sum_{i=1}^{J+1} a_i b_i^n = \mu^n, \quad (2.62)$$

for  $n = 0, 1, \dots, J$ .

For the case of two-dimensional random media in the continuous setting, every measure  $\mu \in \mathcal{M}_J^\mu$  gives rise to a function  $m(h, \mu)$  that is the effective (relative) conductivity of a multi-rank laminate [58]. However, in general [34], not every measure  $\mu \in \mathcal{M}_J^\mu$  gives rise to such a function  $m(h, \mu)$ . Therefore, the set  $A_J^\mu$  will *contain* the exact range of values of the effective conductivity [34]. This is sufficient for the bounding procedure discussed in this section.

By the symmetries between the formulas in equation (2.12), the support of the measure  $\eta$  is contained in the interval  $[0, 1]$  and its mass is given by  $\eta^0 = p_2 = 1 - p_1$ , where  $0 \leq p_2 \leq 1$ . We can therefore define compact, convex sets  $\mathcal{M}_J^\eta \subset \mathcal{M}$  and  $A_J^\eta \subset \mathbb{C}$  which are analogous to those defined in equations (2.60) and (2.61), respectively, involving the function  $\tilde{m}(h, \eta) = 1 - E(s, \eta)$ . Moreover, the extreme points of  $\mathcal{M}_0^\eta$  are the one point measures  $c\delta_d$ ,  $0 \leq c, d \leq 1$ , while the extreme points of  $\mathcal{M}_J^\eta$  are weak limits of convex combinations of measures of the form given in equation (2.62).

Consequently, in order to determine the extreme points of the sets  $A_J^\mu$  and  $A_J^\eta$ , it suffices to determine the range of values in  $\mathbb{C}$  of the functions  $m(h, \mu_J) = 1 - F(s, \mu_J)$

and  $\tilde{m}(h, \eta_J) = 1 - E(s, \eta_J)$ , respectively, where

$$F(s, \mu_J) = \sum_{i=1}^{J+1} \frac{a_i}{s - b_i}, \quad E(s, \eta_J) = \sum_{i=1}^{J+1} \frac{c_i}{s - d_i}, \quad (2.63)$$

as the  $a_i$ ,  $b_i$ ,  $c_i$ , and  $d_i$  vary under the constraints given in equation (2.62). While  $F(s, \mu_J)$  and  $E(s, \eta_J)$  in (2.63) may not run over all points in  $A_J^\mu$  and  $A_J^\eta$  as these parameters vary, they run over the extreme points of these sets, which is sufficient due to their convexity. It is important to note that, as the effective complex conductivity  $\sigma^*$  is given by  $\sigma^* = \sigma_2 m(h, \mu) = \sigma_1 / \tilde{m}(h, \eta)$ , the regions  $A_J^\mu$  and  $A_J^\eta$  have to be mapped to the common  $\sigma^*$ -plane to provide bounds for  $\sigma^*$ .

We will discuss the bounds for  $\sigma^*$  in detail for the cases where  $J=0, 1$ , and briefly explain how the procedure is generalized to obtain a sequence of nested bounds for  $J=2, 3, \dots$  [28]. The bounds corresponding to the case where  $J=0$  follows from the knowledge of only the masses  $\mu^0$  and  $\eta^0$  of the measures  $\mu$  and  $\eta$ . For simplicity, we assume that  $\mu^0 = p_1$  and  $\eta^0 = p_2$ . If the random medium is also known to be statistically isotropic, so that the effective tensors  $\boldsymbol{\sigma}^*$  and  $\boldsymbol{\rho}^*$  are diagonal [58], the first moments  $\mu^1$  and  $\eta^1$  are also known to be given by [28]

$$\mu^1 = \frac{p_1 p_2}{d}, \quad \eta^1 = \frac{p_1 p_2 (d-1)}{d}, \quad (2.64)$$

which leads to bounds for the case where  $J=1$ .

Consider the case where  $J=0$  in (2.63) and the volume fraction  $p_1 = 1 - p_2$  is fixed with  $\mu^0 = p_1$  and  $\eta^0 = p_2$ , so that  $F(s, \mu_J) = p_1 / (s - \lambda)$  and  $E(s, \eta_J) = p_2 / (s - \tilde{\lambda})$ . By the above discussion, the values of  $F(s, \mu)$  and  $E(s, \eta)$  lie inside the circles  $C_0(\lambda)$  and  $\tilde{C}_0(\tilde{\lambda})$ , respectively, given by

$$C_0(\lambda) = \frac{\mu^0}{s - \lambda}, \quad -\infty \leq \lambda \leq \infty, \quad \tilde{C}_0(\tilde{\lambda}) = \frac{\eta^0}{s - \tilde{\lambda}}, \quad -\infty \leq \tilde{\lambda} \leq \infty. \quad (2.65)$$

In the  $\sigma^*$ -plane, the intersection of these two regions is bounded by two circular arcs corresponding to  $0 \leq \lambda \leq p_2$  and  $0 \leq \tilde{\lambda} \leq p_1$  in (2.65), and the values of  $\sigma^*$  lie inside this region [28]. These bounds are optimal [56, 8], and are obtained by a composite of uniformly aligned spheroids of material 1 in all sizes coated with confocal shells of material 2, and vice versa. The arcs are traced out as the aspect ratio varies. When the value of the component conductivities  $\sigma_1$  and  $\sigma_2$  are real and positive, the bounding region collapses to the interval  $1/(p_1/\sigma_1 + p_2/\sigma_2) \leq \sigma^* \leq p_1\sigma_1 + p_2\sigma_2$ , which are the Wiener bounds. The lower and upper bounds are obtained by parallel slabs of the two materials aligned perpendicular and parallel to the field  $\vec{E}_0$ , respectively [72].

Now consider the case where  $J=1$  in (2.63). Here, the volume fraction  $p_1 = 1 - p_2$  is fixed so that  $\mu^0 = p_1$  and  $\eta^0 = p_2$ , and the random medium is statistically isotropic so that the first moments  $\mu^1$  and  $\eta^1$  are given by that in equation (2.64). A convenient way of including this information is to use the transformations [8]

$$F_1(s) = \frac{1}{p_1} - \frac{1}{sF(s)}, \quad E_1(s) = \frac{1}{p_2} - \frac{1}{sE(s)}. \quad (2.66)$$

Due to the symmetries between  $F_1(s)$  and  $E_1(s)$  in (2.66), we will first focus on the function  $F_1(s)$  and introduce the function  $E_1(s)$  when appropriate. The function

$F_1(s)$  is an upper half plane function analytic off  $[0, 1]$  and therefore has an integral representation [8, 28] analogous to that in equation (2.12), involving a measure  $\mu_1$ , say, which is supported in the interval  $[0, 1]$ . Since only the mass  $\mu^0 = p_1$  and the first moment  $\mu^1 = p_1 p_2 / d$  of the measure  $\mu$  are known, the transformation (2.66) determines only the mass  $\mu_1^0 = p_2 / (p_1 d)$  of the measure  $\mu_1$  [8, 28]. This reveals the utility of the transformation  $F_1(s)$  in equation (2.66), it reduces the  $J = 1$  case for  $F(s)$  to the  $J = 0$  case for  $F_1(s)$ .

By our previous analysis, the values of  $F_1(s)$  lie inside a circle  $p_2 / (p_1 d(s - \lambda))$ ,  $-\infty \leq \lambda \leq \infty$ . Similarly, the values of  $E_1(s)$  lie inside a circle  $p_1(d - 1) / (p_2 d(s - \tilde{\lambda}))$ ,  $-\infty \leq \tilde{\lambda} \leq \infty$ . Since  $F$  and  $E$  are fractional linear in  $F_1$  and  $E_1$ , respectively, these circles are transformed to the circles  $C_1(\lambda)$  in the  $F$ -plane and  $\tilde{C}_1(\tilde{\lambda})$  in the  $E$ -plane given by [28]

$$C_1(\lambda) = \frac{p_1(s - \lambda)}{s(s - \lambda - p_2/d)}, \quad \tilde{C}_1(\tilde{\lambda}) = \frac{p_2(s - \tilde{\lambda})}{s(s - \tilde{\lambda} - p_1(d - 1)/d)}, \quad -\infty \leq \lambda, \tilde{\lambda} \leq \infty. \quad (2.67)$$

In the  $\sigma^*$ -plane the intersection of these two circular regions is bounded by two circular arcs [28] corresponding to  $0 \leq \lambda \leq (d - 1)/d$  and  $0 \leq \tilde{\lambda} \leq 1/d$  in (2.67).

The vertices of the region,  $C_1(0) = p_1 / (s - p_2/d)$  and  $\tilde{C}_1(0) = p_2 / (s - p_1(d - 1)/d)$ , are attained by the Hashin–Shtrikman geometries (spheres of all sizes of material 1 in the volume fraction  $p_1$  coated with spherical shells of material 2 in the volume fraction  $p_2$  filling all of  $\mathbb{R}^d$ , and vice versa), and lie on the arcs of the first order bounds [28]. While there are at least five points on the arc  $C_1(\lambda)$  in (2.67) that are attainable by composite microstructures [56], the arc  $\tilde{C}_1(\tilde{\lambda})$  in (2.67) violates [28] the interchange inequality  $m(h)m(1/h) \geq 1$  [50, 73], which becomes an equality in two dimensions [58]. Consequently, the isotropic bounds in (2.67) are not optimal, but have been improved [55, 8] by incorporating the interchange inequality. When  $\sigma_1$  and  $\sigma_2$  are real and positive with  $\sigma_1 \leq \sigma_2$ , the region collapses to the interval

$$\sigma_1 + p_2 \left/ \left( \frac{1}{\sigma_2 - \sigma_1} + \frac{p_1}{d\sigma_1} \right) \right. \leq \sigma^* \leq \sigma_2 + p_1 \left/ \left( \frac{1}{\sigma_1 - \sigma_2} + \frac{p_2}{d\sigma_2} \right) \right., \quad (2.68)$$

which are the Hashin–Shtrikman bounds.

The higher moments  $\mu^n$ , for  $n \geq 2$ , depend on the  $(n + 1)$ -point correlation functions of the medium [34] and have not been calculated in general. Although, the interchange inequality forces relations among them [57]. If the moments  $\mu^0, \dots, \mu^J$  are known, then the transformation  $F_1$  in (2.66) can be iterated to produce an upper half plane function  $F_J$  with a integral representation, involving a positive measure  $\mu_J$  which is supported on the interval  $[0, 1]$ . As in the case where  $J = 1$ , the first  $J$  moments of the measure  $\mu$  determine only the mass  $\mu_J^0$  of the measure  $\mu_J$  [28], and the function  $F_J(s)$  can easily be extremized by the above procedure, and similarly for a function  $E_J(s)$  associated with the moments  $\eta^0, \dots, \eta^J$ . The resulting bounds form a nested sequence of lens-shaped regions [28].

**3. Numerical Results** In Section 2.2.2 we extended the ACM for representing transport in composites to the finite lattice setting. Here, we demonstrate how this mathematical framework can be utilized to compute spectral measures and the associated effective parameters for such two-phase random media. In particular, in the finite lattice setting, the operators  $\Gamma$ ,  $\Upsilon$ , and  $\chi_i$ ,  $i = 1, 2$ , are represented as real-symmetric matrices and the spectral measures of the associated random matrices  $M_i = \chi_i \Gamma \chi_i$

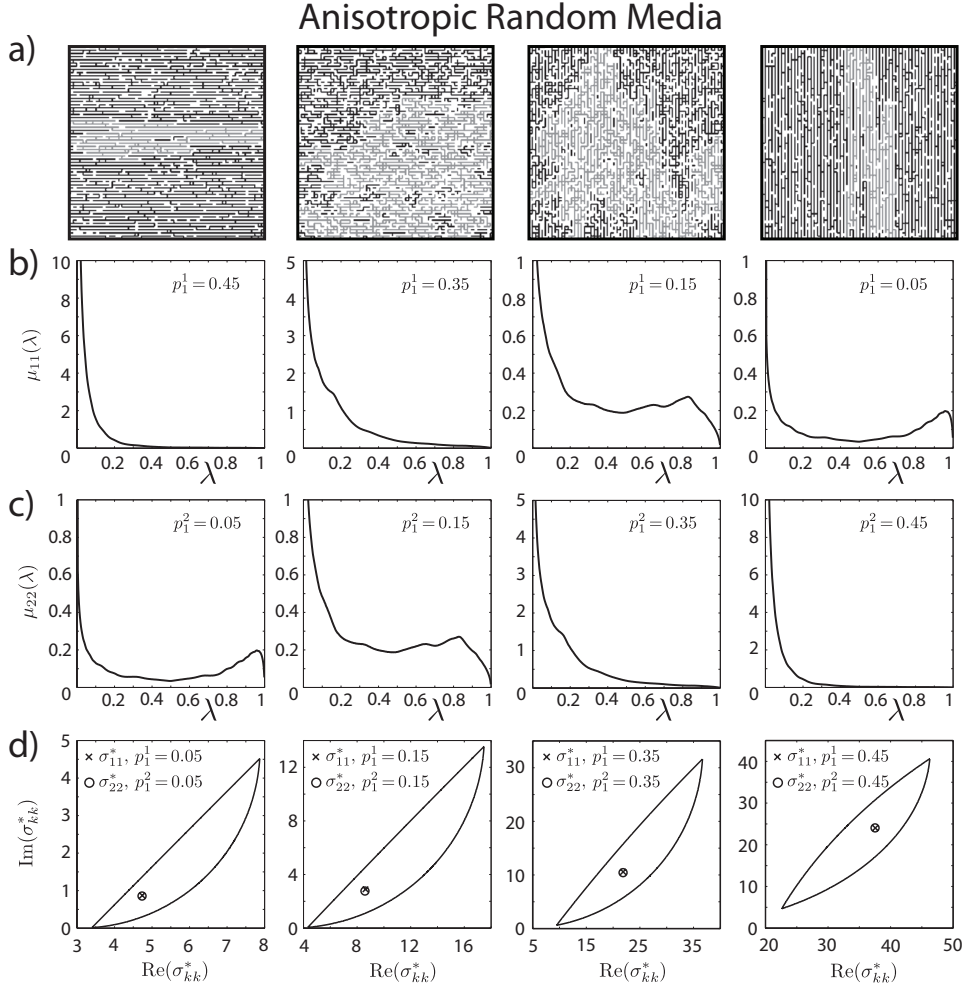


FIG. 3.1. Spectral measures and effective complex conductivities for anisotropic random media. Statistical realizations of the 2D square bond lattice for  $p_1 = 0.5$  and various values of  $p_1^k$ ,  $k = 1, 2$ , are displayed in (a). The type-one bonds are colored black, while the largest connected cluster of type-one bonds is colored grey. The corresponding spectral functions  $\mu_{11}(\lambda)$  and  $\mu_{22}(\lambda)$  are displayed below in (b) and (c), respectively. The effective complex conductivities  $\sigma_{11}^*$  and  $\sigma_{22}^*$  are displayed in (d) for  $p_1^1 = p_1^2$ , along with the associated first-order bounds. The computed spectral functions have been rescaled so that the area under the graph is the measure mass  $\mu_{kk}^0 = dp_1^k$ .

and  $K_i = \chi_i \Upsilon \chi_i$  are explicitly determined by their eigenvalues and eigenvectors, as displayed in equation (2.36). In Section 2.2.2 we also introduced a projection method, summarized by equation (2.58), which provides a numerically efficient way to accomplish these computations. Furthermore, in the paragraph following the statement of Theorem 2.1, we introduced three classes of locally isotropic, statistically isotropic, and anisotropic random media. In this section we employ the projection method to directly calculate the spectral measures and effective parameters for such composite media.

As the system size  $L$  increases, the size  $N = dL^d$  of the matrix  $M_1$ , for example,

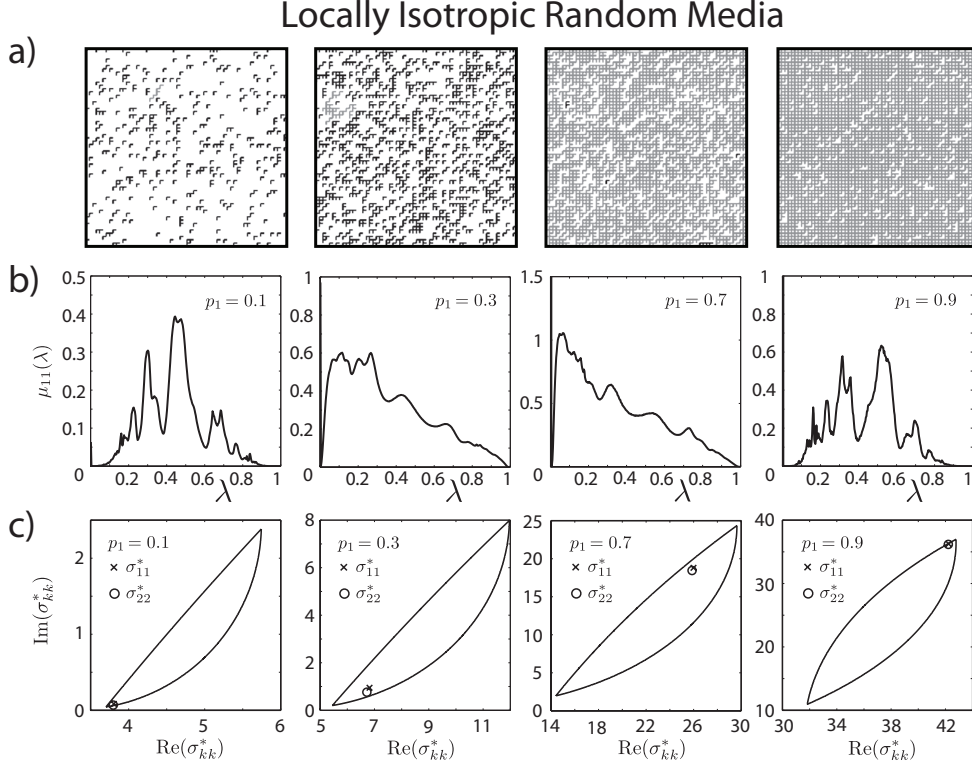


FIG. 3.2. *Spectral measures and effective complex conductivities for locally isotropic random media.* Realizations of the two-dimensional lattice model are displayed in (a). The type-one bonds are colored black, while the largest connected cluster of type-one bonds is colored grey. The corresponding spectral function  $\mu_{11}(\lambda)$  is displayed in (b) and the effective complex conductivity is displayed  $\sigma_{11}^*$  in (c), along with the corresponding isotropic bounds. The computed spectral functions have been rescaled so that the area under the graph is the measure mass  $\mu_{11}^0 = p_1$ .

also increases and its eigenvalues become increasingly dense in the spectral interval  $[0, 1]$ . For a large enough fixed system, or for a random system averaged over many statistical realizations, a high resolution histogram representation of the spectral measure  $\mu_{11}$ , called the *spectral function*  $\mu_{11}(\lambda)$ , begins to resemble a smooth curve, as shown in Figure 3.1.

In Figure 3.1(a) statistical realizations of the anisotropic 2D bond lattice are displayed for  $L = 60$  and a volume (number) fraction  $p_1 = 0.5$  of type-one bonds, with various values of  $p_1^k$ ,  $k = 1, 2$ , the volume fraction of type-one bonds in the positive  $k^{\text{th}}$  direction. In Figure 3.1(b) and (c), we display the behavior of the spectral functions  $\mu_{11}(\lambda)$  and  $\mu_{22}(\lambda)$ , respectively, as  $p_1^k$  varies. In Figure 3.1(d) the computed values of the effective complex conductivities  $\sigma_{11}^*$  and  $\sigma_{22}^*$  are displayed, along with the first order bounds of equation (2.65), which depend only on the mass  $\mu_{kk}^0 = dp_1^k$  of the measure  $\mu_{kk}$  and the value of the contrast parameter  $s = 1/(1 - \sigma_1/\sigma_2)$ . The values of the component conductivities  $\sigma_1$  and  $\sigma_2$  are taken to be that of the brine and pure ice phase, respectively, for a sample of sea ice measured at a frequency of 4.75GHz [4],  $\sigma_1 = 51.0741 + i45.1602$  and  $\sigma_2 = 3.07 + i0.0019$ , yielding  $s \approx -0.034 + i0.032$ . Consistent with the symmetries of the model, these spectral functions and effective complex



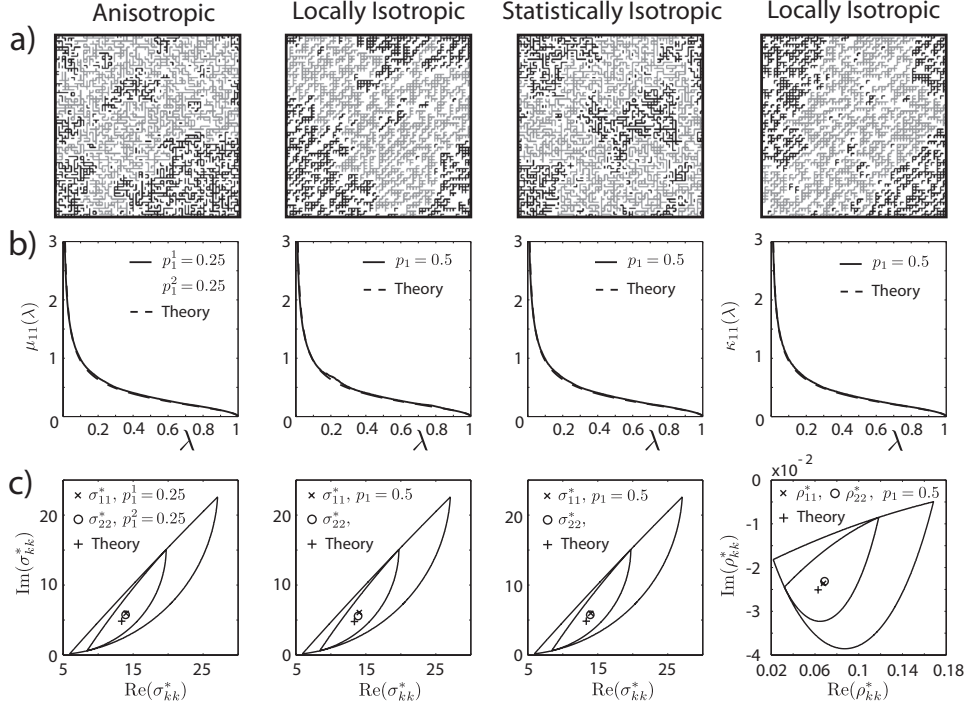


FIG. 3.3. *Statistically self-dual random media.* Realizations of various two-dimensional lattice models are displayed in (a). The type-one bonds are colored black, while the largest connected cluster of type-one bonds is colored grey. The corresponding spectral function  $\mu_{11}(\lambda)$  or  $\kappa_{11}(\lambda)$  is displayed in (b) and the effective complex conductivity  $\sigma_{11}^*$  or resistivity  $\rho_{11}^*$  in (c). In (b) the theoretical prediction for self-dual composite microstructures is also displayed. In (c) the effective complex conductivity or resistivity is displayed along with the theoretical prediction and the first-order and isotropic bounds. The computed spectral functions have been rescaled so that the area under the graph is the measure mass  $\mu_{11}^0 = p_1$ .

conductivities satisfy  $\mu_{11}(\lambda) = \mu_{22}(\lambda)$  and  $\sigma_{11}^* = \sigma_{22}^*$  for  $p_1^1 = p_1^2$ .

We now consider the locally isotropic and statistically isotropic composite classes introduced in the paragraph following the statement of Theorem 2.1. In Figure 3.2 we display the behavior of the spectral function  $\mu_{11}(\lambda)$  and the effective complex conductivity  $\sigma_{11}^*$  as a function of  $p_1$ , for locally isotropic random media with  $L = 60$ . In Figure 3.2(a), statistical realizations of the composite are displayed. These spectral functions exhibit a rich resonance structure. These so called “geometric” resonances have been attributed [47] to the recurrence of local geometric structures called “fractal animals.” In Figure 3.2(c), the corresponding behavior of  $\sigma_{11}^*$  and  $\sigma_{22}^*$  is displayed along with the isotropic bounds of equation (2.67), for the same values of the component conductivities as that in Figure 3.1(c). Consistent with isotropy, the behavior of  $\mu_{22}(\lambda)$  is very similar to that of  $\mu_{11}(\lambda)$  in Figure 3.2(b), and to numerical accuracy and finite size effects we have  $\sigma_{11}^* = \sigma_{22}^*$ . The spectral functions  $\mu_{kk}(\lambda)$ ,  $k=1,2$ , in the case of statistically isotropic random media were computed in [60]. They look very similar to that for the locally isotropic case displayed in Figure 3.2(b). Moreover, the spectral functions  $\kappa_{kk}(\lambda)$ ,  $k=1,2$ , underlying the effective resistivity  $\rho_{kk}^*$ , for locally and statistically isotropic random media also look quite similar to that

## Spectral Measures for 3D Random Resistor Network

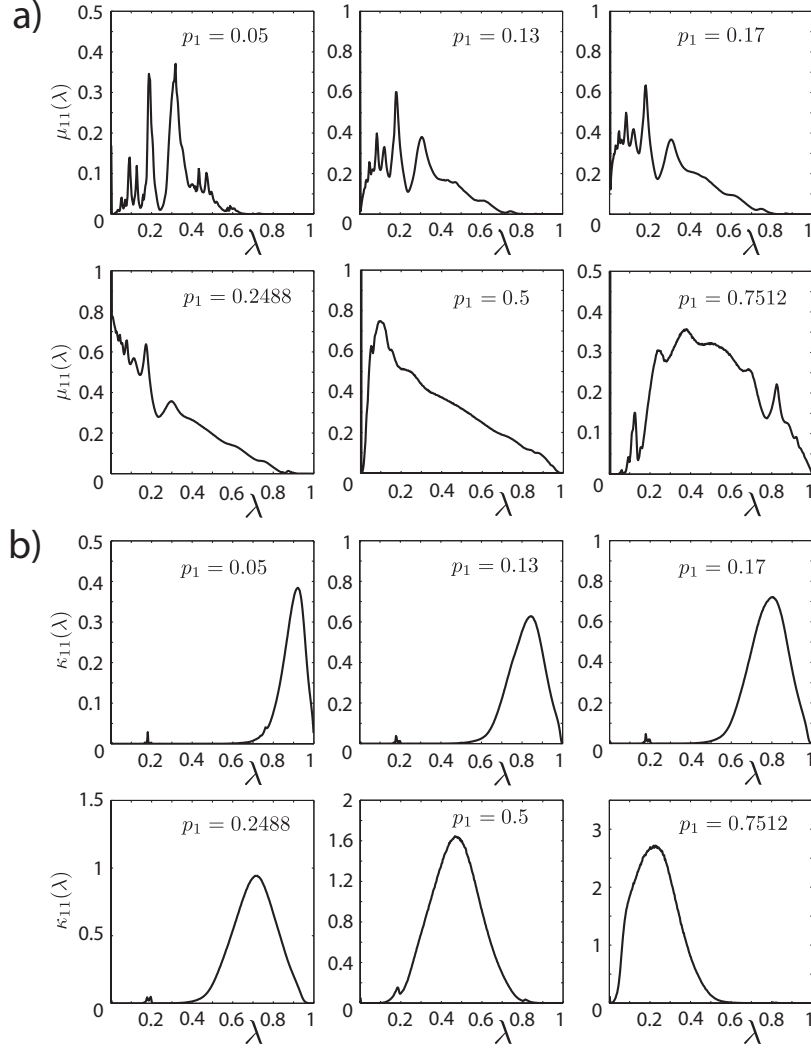


FIG. 3.4. *Spectral measures for 3D locally isotropic random resistor network. For various volume fractions  $p_1$ , the spectral function  $\mu_{11}(\lambda)$  (a) underlying the effective complex conductivity  $\sigma_{11}^*$  is displayed with the spectral function  $\kappa_{11}(\lambda)$  (b) underlying the effective complex resistivity  $\rho_{11}^*$ . The spectral functions have been rescaled so that the area under the graph is the measure mass  $\mu_{11}^0 = \kappa_{11}^0 = p_1$ .*

for  $\mu_{11}(\lambda)$  in Figure 3.2(b).

In the infinite lattice setting, the statistically and locally isotropic composite microstructures are statistically self-dual for  $d=2$  and  $p_1=0.5$  [58]. Note that the class of anisotropic random media for the special case of  $p_1^k = p_1/d$  for all  $k=1, \dots, d$  is statistically isotropic, and is statistically self-dual for  $d=2$  and  $p_1=0.5$ . For such systems, the spectral measures and effective parameters may be explicitly calculated [58], e.g.  $d\mu_{11}(\lambda) = (\sqrt{(1-\lambda)/\lambda})(d\lambda/\pi)$  and  $\sigma_{11}^* = \sqrt{\sigma_1\sigma_2}$ . In Figure 3.3 the computed spec-

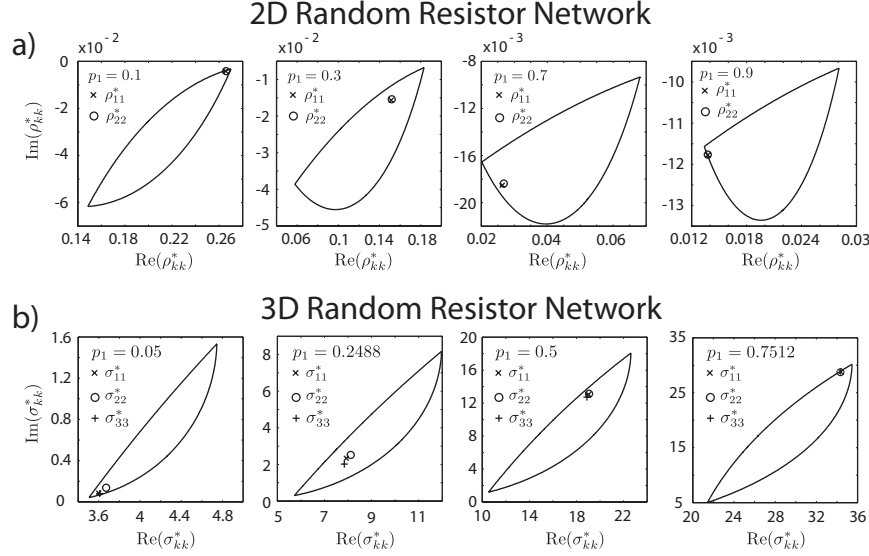


FIG. 3.5. Effective complex parameters and isotropic bounds for 2D and 3D locally isotropic random resistor network (RRN). The behavior of the effective complex resistivity  $\rho_{kk}^*$ ,  $k=1,2$ , for 2D RRN is displayed in (a) for various volume fractions  $p_1$ , along with the corresponding isotropic bounds. Similarly, the behavior of the effective complex conductivity  $\sigma_{kk}^*$ ,  $k=1,2,3$ , and the corresponding isotropic bounds are displayed for 3D RRN in (b).

tral functions and effective parameters are displayed for such random media in the *finite* lattice setting for  $L = 60$ , and compared with the theoretical predictions (for the *infinite* setting). In Figure 3.3(a), the bond color scheme for the displayed statistical realizations is the same as that for Figure 3.1(a). In Figure 3.3(b), the computed spectral functions are displayed along with the theoretical prediction. In Figure 3.3(c) the computed effective parameters are displayed with the theoretical prediction, as well as the first-order and isotropic bounds of equations (2.65) and (2.67), respectively, with the same component conductivities as that in Figure 3.1(c). The computed spectral functions and effective parameters are in excellent agreement with the theoretical predictions for infinite systems. The error in the computed values of the effective parameters, relative to the theoretical prediction, is typically  $\lesssim 10^{-2}$  for  $L = 60$  and decreases as  $L$  increases.

We now discuss the gap behavior of the spectral measures. In the infinite lattice setting, the isotropic composite microstructures discussed in this section are examples of percolation models, which depend only on the volume fraction  $p_1 = 1 - p_2$  of the constituents, hence  $m(h) = m(p_1, h)$ , for example. In these lattice percolation models [77, 80], the bonds are open with probability  $p_1$ , say, and closed with probability  $p_2$ . Connected sets of open bonds are called open clusters. The average cluster size grows as  $p_1$  increases, and there is a critical probability  $p_c$ ,  $0 < p_c < 1$ , called the *percolation threshold*, where an infinite cluster of open bonds first appears. For the two-dimensional lattice percolation model  $p_c = 0.5$  and in three-dimensions  $p_c \approx 0.2488$  [77, 80]. Now consider transport through the associated RRN, where the bonds are assigned electrical conductivities  $\sigma_1$  with probability  $p_1$  and  $\sigma_2$  with probability  $p_2$ . The effective conductivity  $\sigma^*(p_1, h)$ , for example, exhibits two types of critical behavior as  $h = \sigma_1/\sigma_2 \rightarrow 0$ . First, when  $\sigma_1 \rightarrow 0$  and  $0 < \sigma_2 < \infty$ ,  $\sigma^* = 0$  for  $p_1 > p_c$  while

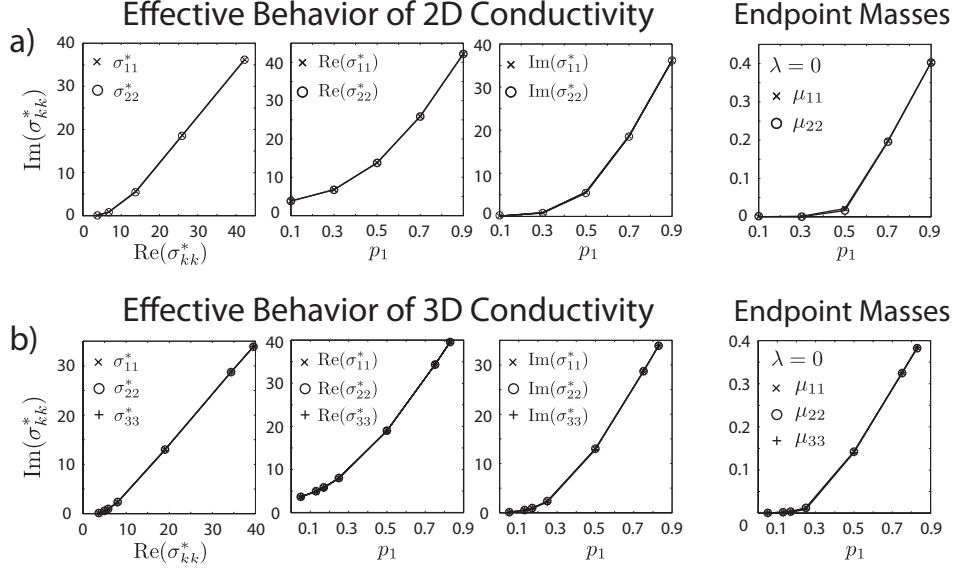


FIG. 3.6. Behavior of the diagonal components  $\sigma_{kk}^*$ ,  $k=1, \dots, d$ , of the effective complex conductivity tensor as a function of volume fraction  $p_1$  for 2D (a) and 3D (b) locally isotropic random resistor network. The corresponding mass of the spectral measure  $\mu_{kk}$  concentrated at  $\lambda=0$  is displayed in (c) and (d), respectively.

$\sigma^* > 0$  for  $p_1 < p_c$ . Second, when  $\sigma_2 \rightarrow \infty$  and  $0 < \sigma_1 < \infty$ ,  $\sigma^*(p_1, 0) \rightarrow \infty$  as  $p_1 \rightarrow p_c^+$ .

First we consider the two-dimensional lattice percolation model. In Figures 3.2(b) and 3.3(b) we see that, as  $p_1$  increases from zero and the system becomes increasingly connected, gaps in the spectral function  $\mu_{11}(\lambda)$  at the spectral endpoints  $\lambda=0, 1$  shrink and then vanish symmetrically at a value of  $p_1 = p_c = 0.5$ . Figure 3.3(b) indicates that the vanishing of the gaps in the spectral function lead to a buildup in the mass of the measure at  $\lambda=0$ , while the mass of the measure is approximately zero for  $\lambda=1$ , i.e.,  $\mu_{11}(1) \approx 0$ .

Now consider the three-dimensional percolation model. In Figure 3.4(a) and (b) we display the behavior of the spectral functions  $\mu_{11}(\lambda)$  and  $\kappa_{11}(\lambda)$  as  $p_1$  varies, for locally isotropic RRN with  $L=15$ . Like its 2D counterpart, the spectral function  $\mu_{11}(\lambda)$  has a rich resonant structure. Furthermore, as  $p_1$  increases from zero and approaches the percolation threshold  $p_c \approx 0.2488$ , a gap in  $\mu_{11}(\lambda)$  about  $\lambda=0$  shrinks and then vanishes, leading to a buildup in the mass of the measure  $\mu_{11}$  at  $\lambda=0$  for  $p_1 = p_c$ . As  $p_1$  increases beyond  $p_c$ , the mass of  $\mu_{11}$  at  $\lambda=0$  continues to grow, while a gap in the spectral function at  $\lambda=1$  shrinks and then vanishes for  $p_1 = 1 - p_c \approx 0.7512$ , with  $\mu_{11}(1) \approx 0$ . The associated behavior of the effective complex conductivity  $\sigma_{kk}^*$ ,  $k=1, 2, 3$ , for the 3D RRN and its corresponding bounds are displayed in Figure 3.5, as well as the effective complex resistivity  $\rho_{kk}^*$ ,  $k=1, 2$ , for the 2D locally isotropic RRN, with the same component conductivities as that of Figure 3.1(c). Consistent with isotropy, to numerical accuracy and finite size effects, we have  $\sigma_{jj}^* = \sigma_{kk}^*$  and  $\rho_{jj}^* = \rho_{kk}^*$  for all  $j, k=1, \dots, d$ . The spectral measures for *statistically isotropic* 3D RRN were computed in [60] and have a very similar behavior to that for locally isotropic RRN displayed in Figure 3.4(a).

The behavior of the spectral function  $\kappa_{11}(\lambda)$  displayed in Figure 3.4(b) has a

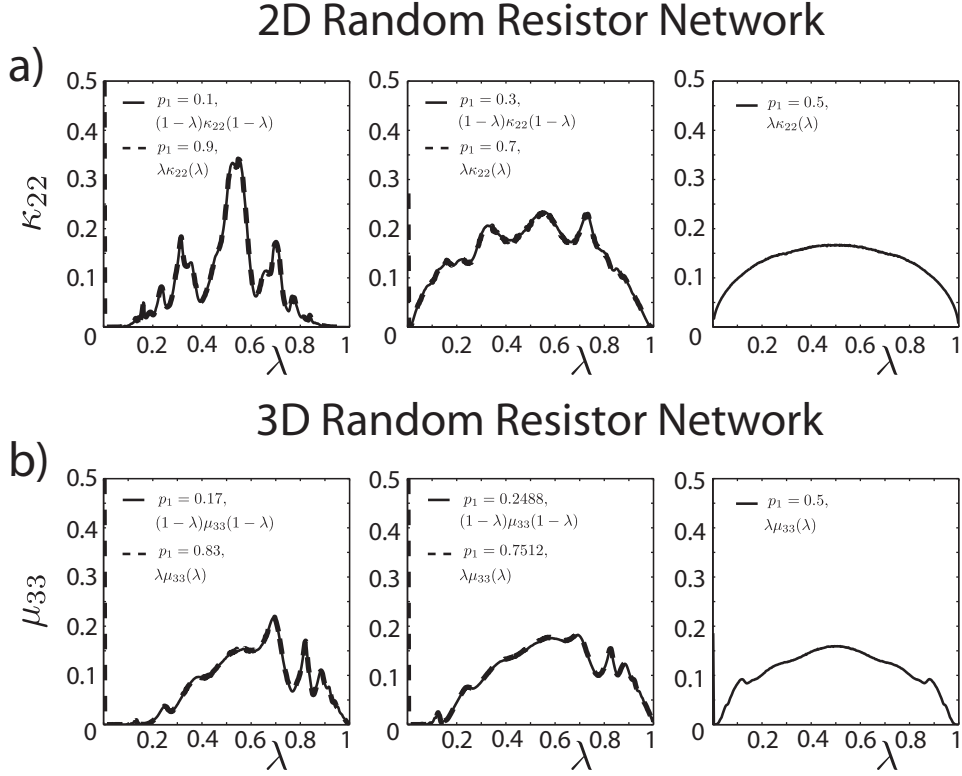


FIG. 3.7. *Spectral measure symmetries. Transformations of the computed spectral functions for 2D (a) and 3D (b) random resistor network, for various values of the volume fraction  $p_1$ . The computed spectral functions have been rescaled to make the area under the graph the measure mass.*

similar gap behavior. For a volume fraction of  $p_1 = 0.001$  (not shown) there is a clear gap in the spectral function about  $\lambda = 0$  and  $\lambda = 1$ . The gap near  $\lambda = 1$  collapses as  $p_1 \rightarrow p_c$ , with  $\kappa_{11}(1) \approx 0$ . As  $p_1$  surpasses  $p_c$  and approaches  $1 - p_c$  the gap in the spectral function near  $\lambda = 0$  collapses, causing a buildup in the mass of the measure at  $\lambda = 0$  as  $p_1 \rightarrow 1 - p_c$ .

Displayed in Figure 3.6 is the behavior of the diagonal components  $\sigma_{kk}^*$ ,  $k = 1, \dots, d$ , of the effective complex conductivity tensor as a function of volume fraction  $p_1$ , for 2D (a) and 3D (b) locally isotropic RRN. The respective masses of the measures  $\mu_{kk}$ ,  $k = 1, \dots, d$ , concentrated at the spectral endpoint  $\lambda = 0$  are displayed in (c) and (d). The component conductivities are the same as that in Figure 3.1(c). It can be seen in Figure 3.6 (c) and (d) that for  $p_1 < p_c$  a very small fraction of the measure mass is concentrated at  $\lambda = 0$ , where  $p_c = 0.5$  for 2D and  $p_c \approx 0.2488$  for 3D. While as  $p_1$  surpasses  $p_c$ , a significant amount of the measure mass becomes concentrated at the spectral endpoint  $\lambda = 0$ . This  $\delta$ -function behavior in the measure at  $\lambda = 0$  leads to significant changes in  $\sigma_{kk}^*$  as the volume fraction  $p_1$  surpasses  $p_c$ , as can be seen in this figure. The associated mass of  $\mu_{kk}$  concentrated at  $\lambda = 1$  is  $\sim 10^{-30}$  for both 2D and 3D.

This behavior in the spectral measures is consistent with equation (2.14), which holds for general stationary random media in the infinite setting [60], and consequently

holds for percolation models of such media. This equation characterizes the percolation transition with the formation of delta components in the spectral measures at the spectral endpoints  $\lambda = 0, 1$ , *precisely* at  $p_1 = p_c$  and  $p_1 = 1 - p_c$ . Recall that the weights  $m_{kk}(0)$  and  $w_{kk}(0)$  of the delta components at  $\lambda = 0$  and  $\lambda = 1$  in (2.14), for example, have the following behavior. When  $\sigma_1 = 0$  ( $h = 0$ ), the function  $m_{kk}(0) = m_{kk}(p_1, 0)$ ,  $k = 1, \dots, d$ , increases from zero as  $p_1$  surpasses  $p_c$  ( $p_1 \rightarrow p_c^+$ ). Similarly, when  $\sigma_2 = 0$  ( $z = 0$ ), the function  $w_{kk}(0) = w_{kk}(p_2, 0)$  increases from zero as  $p_1$  surpasses  $1 - p_c$  ( $p_1 \rightarrow 1 - p_c^-$ ). For conductor/insulator or conductor/superconductor systems, this behavior in the spectral endpoints of the measures lead to critical behavior in the effective conductivity [60, 30].

Equation (2.14) also provides a relationship between the measures  $\mu_{jk}$  and  $\alpha_{jk}$ , and the measures  $\eta_{jk}$  and  $\kappa_{jk}$ . In Figure 3.7 we demonstrate that this relationship between the spectral measures persists in the finite lattice setting. Displayed in Figure 3.7(a) are graphs of transformations of the spectral function  $\kappa_{22}(\lambda)$ . In particular, the graph of the function  $(1 - \lambda)\kappa_{22}(1 - \lambda)$  is displayed for volume fractions  $p_1 = 0.1, 0.3$ , and  $0.5$ , along with  $\lambda\kappa_{22}(\lambda)$  for a volume fraction of  $1 - p_1$ . Similarly, in Figure 3.7(b) the graphs of  $(1 - \lambda)\mu_{33}(1 - \lambda)$  and  $\lambda\mu_{33}(\lambda)$  are displayed for various values of  $p_1$  and  $1 - p_1$ , respectively. The graphs of the transformed spectral functions are virtually identical except for a “delta function” at  $\lambda = 0$ , in excellent agreement with equation (2.14), which holds for infinite systems.

**4. Conclusion** In Sections 2.1 and 2.2.1 we reviewed and extended the ACM for representing transport in two-phase random media, for the *infinite* continuum and lattice settings, respectively. This method provides the Stieltjes integral representations displayed in equation (2.12) for the effective transport coefficients of such composite media, which involve spectral measures associated with the self-adjoint random operators  $M_i = \chi_i \Gamma \chi_i$  and  $K_i = \chi_i \Upsilon \chi_i$ . Here,  $\chi_i$  is the characteristic function for material phase  $i = 1, 2$  and the operators  $\Gamma = \vec{\nabla}(\Delta^{-1})\vec{\nabla}$  and  $\Upsilon = -\vec{\nabla} \times (\Delta^{-1})\vec{\nabla} \times$  act as projectors onto curl-free and divergence-free fields, respectively.

In Section 2.2.2 we developed the ACM for representing transport in two-phase random media, with *finite* lattice composite microstructure. This novel formulation yields discrete Stieltjes integral representations for the effective transport coefficients of such media, displayed in equation (2.36) of Theorem 2.1, which is a key theoretical contribution of this work. We accomplished this by developing a novel formulation of the ACM in Section 2.2.3, that is equivalent to the original formulation [34], which holds for both the finite lattice setting and the infinite, continuum and lattice settings. We also provided a projection method for numerically efficient, rigorous computation of spectral measures and effective parameters for composite media with finite lattice microstructure. This projection method is summarized by equations (2.56)–(2.58). In this finite lattice case, the operators  $\chi_i$ ,  $\Gamma$ , and  $\Upsilon$  are represented by real-symmetric projection matrices, and the spectral measures of the associated real-symmetric random matrices  $M_i$  and  $K_i$  are given explicitly in terms of their eigenvalues and eigenvectors, as displayed in equation (2.36).

In Section 2.2.2, following the statement of Theorem 2.1, we introduced three families of locally isotropic, statistically isotropic, and anisotropic random media with finite lattice composite microstructure. In Section 3 we employed the projection method to compute the spectral measures and effective parameters associated with these families of random media. To our knowledge, this is the first time that the spectral measures  $\eta_{jk}$  and  $\kappa_{jk}$  underlying the effective complex resistivity  $\rho_{jk}^*$  have been computed for such composite microstructures. These computations not

only demonstrate several important properties of the spectral measures and effective parameters, but they also serve as a consistency check to the theory developed here.

The computed spectral functions and effective complex parameters for anisotropic random media, displayed in Figure 3.1, are consistent with the symmetries of the model. Consistent with general theory [58], our computations of the effective parameters for isotropic random media satisfy  $\sigma_{kk}^* = 1/\rho_{kk}^*$ ,  $k = 1, \dots, d$  (to numerical accuracy and statistical truncation). Moreover, the computed spectral functions and effective parameters are consistent with isotropy and satisfy  $\mu_{jj}(\lambda) = \mu_{kk}(\lambda)$  and  $\sigma_{jj}^* = \sigma_{kk}^*$ , for example, for all  $j, k = 1, \dots, d$  (to numerical accuracy, finite size effects, and statistical truncation). Figure 3.3 demonstrates that the projection method accurately calculates the spectral measures and effective parameters for statistically self-dual composite microstructures. Furthermore, Figure 3.7 shows that the computed spectral measures are in excellent agreement with equation (2.14), which holds for general stationary two-phase random media [60].

The self-consistent mathematical framework developed here helps lay the groundwork for studies in the effective transport properties of a broad range of important composites, such as electrorheological fluids [63], multiscale sea ice structures [62], and bone [33]. Remarkably, the ACM has also been adapted to provide Stieltjes integral representations for effective transport coefficients underlying a wide variety of transport processes, such as: the effective diffusivity for steady [52, 2, 65] and time-dependent [3, 64] fluid velocity fields, the effective complex permittivity for uniaxial polycrystalline media [5, 38, 59], and the effective elastic moduli of two-phase elastic composites [68, 67]. The Golden-Papanicolaou formulation of the ACM has been pivotal in the development of these mathematical frameworks, and in the understanding of these important transport processes.

**A-1. Appendix: The Spectral Theorem** In equations (2.12) and (2.36) of Sections 2.1 and 2.2.2, we display integral representations for the functions  $F_{jk}(s)$  and  $G_{jk}(t)$ ,  $j, k = 1, \dots, d$ , involving spectral measures  $\mu_{jk}$  and  $\alpha_{jk}$  associated with the operators  $M_i = \chi_i \Gamma \chi_i$ ,  $i = 1, 2$ , as well as that for the functions  $E_{jk}(s)$  and  $H_{jk}(t)$  involving spectral measures  $\eta_{jk}$  and  $\kappa_{jk}$  associated with the operators  $K_i = \chi_i \Upsilon \chi_i$ ,  $i = 1, 2$ . In this section, we discuss the spectral theorem as it pertains to the ACM, which provides the existence of these Stieltjes integral representations. The abstract, bounded linear self-adjoint operator case [70, 79], associated with the infinite, continuum and lattice settings, is discussed in Section A-1.1. While the real-symmetric matrix case [51, 39, 76], associated with the finite lattice setting, is discussed in Section A-1.2. Since the formulations associated with each of the operators  $M_i = \chi_i \Gamma \chi_i$  and  $K_i = \chi_i \Upsilon \chi_i$ ,  $i = 1, 2$ , are analogous, for simplicity, we will focus on that for the operator  $M_1 = \chi_1 \Gamma \chi_1$ . Also, in Section 2.2.3 we provided a novel formulation of the ACM involving the operator  $M_1$ , which is equivalent to the original formulation [34, 10] involving the operator  $\Gamma \chi_1$ , and holds for both the finite lattice setting and the infinite, continuum and lattice settings. Due to this unification, we will focus on the formulation of the ACM associated with the operator  $M_1$ .

**A-1.1. Infinite Continuum and Lattice Settings** In this section, we review the spectral theorem as it pertains to the ACM for the infinite, continuous and lattice settings. Consider the Hilbert space  $\mathcal{H}_\infty$  defined in equation (2.2). Now, define the Hilbert space  $\mathcal{H}_0 = \mathcal{H}_\infty \cup \mathbb{C}^d$  by

$$\mathcal{H}_0 = \left\{ \vec{Y} \in \mathcal{H} \mid \vec{\nabla} \times \vec{Y} = 0 \text{ weakly} \right\}, \quad (\text{A-1})$$

where  $\vec{\nabla} \times \vec{Y} = 0$  means that  $L_i Y_j - L_j Y_i = 0$  for all  $i, j = 1, \dots, d$ . In other words,  $\mathcal{H}_0$  is the Hilbert space  $\mathcal{H}_\times$  with the constant fields  $\mathbb{C}^d$  included. Equip  $\mathcal{H}_0$  with the  $\mathcal{H}$ -inner-product weighted by the characteristic function  $\chi_1$ , which we denote by  $\langle \cdot, \cdot \rangle_1$ . In the infinite, continuum and lattice settings, the characteristic function acts *pointwise* on the underlying vector space,  $\mathbb{R}^d$  or  $\mathbb{Z}^d$ , and it is therefore a self-adjoint operator on  $\mathcal{H}_0$ . Clearly, it is also a linear projection operator satisfying  $\langle \chi_1 \vec{\xi}, \vec{\zeta} \rangle = \langle \chi_1^2 \vec{\xi}, \vec{\zeta} \rangle$  for all  $\vec{\xi}, \vec{\zeta} \in \mathcal{H}_0$ , and is therefore bounded on  $\mathcal{H}_0$  with operator norm  $\|\chi_1\| \leq 1$ .

On  $L^2(\Omega, P)$ , the linear operator  $\Delta^{-1}$  is bounded and self-adjoint [76]. For all  $\vec{\xi} \in \mathcal{H}_0$  we have  $\vec{\nabla} \cdot \vec{\xi} \in L^2(\Omega, P)$ , and for all  $\vec{\zeta} \in L^2(\Omega, P)$  we have  $\|\vec{\nabla} \Delta^{-1} \vec{\zeta}\| < \infty$ , where  $\|\cdot\|$  denotes the norm induced by the  $\mathcal{H}$ -inner-product. It follows that the linear operator  $\Gamma = \vec{\nabla}(\Delta^{-1})\vec{\nabla} \cdot$  is bounded on  $\mathcal{H}_0$ . Integration by parts then establishes that  $\Gamma$  is self-adjoint on  $\mathcal{H}_0$  [34]. It is also clear that  $\Gamma$  is a projection operator satisfying  $\langle \Gamma \vec{\xi}, \vec{\zeta} \rangle = \langle \Gamma^2 \vec{\xi}, \vec{\zeta} \rangle$  for all  $\vec{\xi}, \vec{\zeta} \in \mathcal{H}_0$ , with operator norm  $\|\Gamma\| \leq 1$ .

It follows that  $M_1 = \chi_1 \Gamma \chi_1$  is a bounded linear self-adjoint operator on the Hilbert space  $\mathcal{H}_0$ , with operator norm  $\|M_1\| \leq 1$  [70, 79]. The spectrum  $\Sigma$  of the self-adjoint operator  $M_1$  is real-valued and the spectral radius of  $M_1$  is equal to its operator norm [70], which implies that  $\Sigma \subseteq [-1, 1]$ . However, since  $\chi_1$  and  $\Gamma$  are self-adjoint projection operators on  $\mathcal{H}_0$ , we have  $\langle \chi_1 \Gamma \chi_1 \vec{\xi}, \vec{\xi} \rangle = \langle \Gamma \chi_1 \vec{\xi}, \Gamma \chi_1 \vec{\xi} \rangle = \|\Gamma \chi_1 \vec{\xi}\|^2 \geq 0$  for all  $\vec{\xi} \in \mathcal{H}_0$ . This implies that  $M_1$  is also a positive operator, which implies that its spectrum satisfies  $\Sigma \subseteq [0, \infty)$  [79]. Consequently, the spectrum  $\Sigma$  of  $M_1$  satisfies  $\Sigma \subseteq [0, 1]$ .

Since  $\Sigma \subseteq [0, 1]$ , the spectral theorem for bounded linear self-adjoint operators in Hilbert space [79] states that there is a one-to-one correspondence between the operator  $M_1$  and a family of self-adjoint projection operators  $\{Q(\lambda)\}_{\lambda \in [0, 1]}$  — the resolution of the identity — that satisfies  $\lim_{\lambda \rightarrow 0} Q(\lambda) = 0$  and  $\lim_{\lambda \rightarrow 1} Q(\lambda) = I$ , where 0 and  $I$  are the null and identity operators on  $\mathbb{R}^d$ . Furthermore, for all  $\vec{\xi}, \vec{\zeta} \in \mathcal{H}_0$ , the function of  $\lambda$  defined by  $\mu_{\xi\zeta}(\lambda) = \langle Q(\lambda) \vec{\xi}, \vec{\zeta} \rangle_1$  is strictly increasing and of bounded variation, and therefore has a Stieltjes measure  $\mu_{\xi\zeta}$  associated with it [78, 79, 26]. The spectral theorem also states that, for all complex valued functions  $f \in L^2(\mu_{\xi\zeta})$ , there exists a linear operator denoted by  $f(M_1)$  which is defined in terms of the functional  $\langle f(M_1) \vec{\xi}, \vec{\zeta} \rangle_1 = \langle f(M_1) \chi_1 \vec{\xi}, \vec{\zeta} \rangle$ . Moreover, this functional has the following integral representation involving the Stieltjes measure  $\mu_{\xi\zeta}$

$$\langle f(M_1) \vec{\xi}, \vec{\zeta} \rangle_1 = \int_0^1 f(\lambda) d\mu_{\xi\zeta}(\lambda), \quad \mu_{\xi\zeta}(\lambda) = \langle Q(\lambda) \vec{\xi}, \vec{\zeta} \rangle_1, \quad (\text{A-2})$$

where the integration is over the spectrum  $\Sigma$  of  $M_1$  [70, 79]. Setting  $f(\lambda) = (s - \lambda)^{-1}$  for  $s \in \mathbb{C} \setminus [0, 1]$ ,  $\vec{\xi} = \vec{e}_j$ , and  $\vec{\zeta} = \vec{e}_k$  in equation (A-2), yields the integral formula for  $F_{jk}(s)$  displayed in equation (2.44), which is equivalent to that displayed in (2.12).

**A-1.2. Finite Lattice Setting** In this section, we review the spectral theorem as it pertains to the ACM for the finite lattice setting discussed in Section 2.2.2. In this case, the operator  $M_1 = \chi_1 \Gamma \chi_1$  is represented by a real-symmetric random matrix and the spectral theorem for such matrices provides a discrete version of the integral representation displayed in equation (A-2). This formulation leads to the discrete integral representation of the function  $F_{jk}(s)$  displayed in equations (2.36) and (2.44).

Recall that we defined in Section 2.2.2 a bijective mapping  $\Theta: \mathbb{Z}_L^d \rightarrow \mathbb{N}_L$  from the finite  $d$ -dimensional bond lattice  $\mathbb{Z}_L^d$  of size  $L$  onto the one dimensional set  $\mathbb{N}_L$  of size  $N = dL^d$ . Moreover, we showed that, under the mapping  $\Theta$ , the random operator  $M_1 = \chi_1 \Gamma \chi_1$  can be represented by a random matrix of size  $N \times N$  [33, 60]. More specifically,  $\Gamma$  is a *non-random*, real-symmetric projection matrix satisfying  $\Gamma^2 = \Gamma$ .



Consequently,  $\|\Gamma\| \leq 1$ , where  $\|\cdot\|$  denotes the matrix norm induced by the dot-product on  $\mathbb{C}^N$  [23]. In this finite lattice setting, the characteristic function  $\chi_1$  is represented by a *random*, diagonal projection matrix satisfying  $\chi_1^2 = \chi_1$ , with zeros and ones along its diagonal. Consequently, the matrix  $\chi_1$  is real-symmetric and satisfies  $\|\chi_1\| \leq 1$ .

It follows that  $M_1$  is a real-symmetric matrix with  $\|M_1\| \leq 1$  [23]. It is also a composition of projection matrices, and is consequently positive definite, i.e., for every  $\vec{\xi} \in \mathbb{C}^N$  we have that  $\chi_1 \Gamma \chi_1 \vec{\xi} \cdot \vec{\xi} = (\Gamma \chi_1 \vec{\xi}) \cdot (\Gamma \chi_1 \vec{\xi}) \geq 0$ . This, implies that the spectrum  $\Sigma$  of  $M_1$  is comprised of real eigenvalues  $\lambda_i$ ,  $i = 1, \dots, N$ , and that  $\Sigma \subseteq [0, \infty)$  [45]. Furthermore, the largest eigenvalue of the matrix  $M_1$  is equal to  $\|M_1\|$  [23]. It follows that  $\Sigma \subseteq [0, 1]$ .

It is well known [45, 49] that the eigenvectors  $\vec{u}_i$ ,  $i = 1, \dots, N$ , of the real-symmetric matrix  $M_1$  form an orthonormal basis for  $\mathbb{R}^N$ , i.e.,  $\vec{u}_\ell^T \vec{u}_m = \delta_{\ell m}$  and for every  $\vec{\xi} \in \mathbb{R}^N$  we have  $\vec{\xi} = \sum_{i=1}^N (\vec{u}_i^T \vec{\xi}) \vec{u}_i = \left( \sum_{i=1}^N \vec{u}_i \vec{u}_i^T \right) \vec{\xi}$ . Consequently,

$$\sum_{i=1}^N Q_i = I, \quad Q_i = \vec{u}_i \vec{u}_i^T, \quad Q_\ell Q_m = Q_\ell \delta_{\ell m}, \quad (\text{A-3})$$

where  $I$  is the identity matrix on  $\mathbb{R}^N$ . Here, we have defined  $Q_i$ ,  $i = 1, \dots, N$ , to be the mutually orthogonal projection matrices onto the eigenspaces spanned by the  $\vec{u}_i$ .

Since  $M_1 \vec{u}_i = \lambda_i \vec{u}_i$ , the identity  $Q_i = \vec{u}_i \vec{u}_i^T$  implies that we also have  $M_1 Q_i = \lambda_i Q_i$ . This and equation (A-3) then imply that the matrix  $M_1$  has the spectral decomposition  $M_1 = \sum_{i=1}^N \lambda_i Q_i$ . By the mutual orthogonality of the projection matrices  $Q_i$  and by induction, we have that  $M_1^n = \sum_{i=1}^N \lambda_i^n Q_i$  for all  $n \in \mathbb{N}$ . This, in turn, implies that  $f(M_1) = \sum_{i=1}^N f(\lambda_i) Q_i$  for any polynomial  $f: \mathbb{R} \mapsto \mathbb{C}$ . Consequently, for all  $\vec{\xi}, \vec{\zeta} \in \mathbb{C}^N$ , the functional  $\langle f(M_1) \vec{\xi} \cdot \vec{\zeta} \rangle_1 = \langle f(M_1) \chi_1 \vec{\xi} \cdot \vec{\zeta} \rangle$  has the following integral representation

$$\langle f(M_1) \vec{\xi} \cdot \vec{\zeta} \rangle_1 = \int_0^1 f(\lambda) d\mu_{\xi\zeta}(\lambda), \quad d\mu_{\xi\zeta}(\lambda) = \sum_{i=1}^N \langle \delta_{\lambda_i}(d\lambda) Q_i \vec{\xi} \cdot \vec{\zeta} \rangle_1. \quad (\text{A-4})$$

The proof of Theorem 2.1 given in Section 2.2.4 demonstrates that equation (A-4) also holds for the function  $f(\lambda) = (s - \lambda)^{-1}$  when  $s \in \mathbb{C} \setminus [0, 1]$ . In this matrix setting, the projection valued operator  $Q(\lambda)$  associated with the strictly increasing function  $\mu_{\xi\zeta}(\lambda) = \langle Q(\lambda) \vec{\xi} \cdot \vec{\zeta} \rangle_1$ , discussed in Section A-1.1, can be written explicitly as

$$Q(\lambda) = \sum_{i: \lambda_i < \lambda} \theta(\lambda - \lambda_i) Q_i. \quad (\text{A-5})$$

Here,  $\theta(\lambda)$  is the Heaviside function which takes the value  $\theta(\lambda) = 0$  for  $\lambda < 0$  and  $\theta(\lambda) = 1$  for  $\lambda > 0$  [49].

**Acknowledgments.** We gratefully acknowledge support from the Division of Mathematical Sciences and the Office of Polar Programs at the U.S. National Science Foundation (NSF) through Grants DMS-1009704, ARC-0934721, and DMS-0940249. We are also grateful for support from the Office of Naval Research (ONR) through Grants N00014-13-10291 and N00014-12-10861. Finally, we would like to thank the NSF Math Climate Research Network (MCRN) for their support of this work.

## REFERENCES

- [1] N. I. AKHIEZER, *The Classical Moment Problem*, Oliver & Boyd, 1965.
- [2] M. AVELLANEDA AND A. MAJDA, *An integral representation and bounds on the effective diffusivity in passive advection by laminar and turbulent flows*, Comm. Math. Phys., 138 (1991), pp. 339–391.
- [3] M. AVELLANEDA AND M. VERGASSOLA, *Stieltjes integral representation of effective diffusivities in time-dependent flows*, Phys. Rev. E, 52 (1995), pp. 3249–3251.
- [4] L. G. E. BACKSTROM, *Capacitance Measurements of Bulk Salinity and Brine Movement in First-year Sea Ice*, University of Alaska Fairbanks, 2007.
- [5] S. BARABASH AND D. STROUD, *Spectral representation for the effective macroscopic response of a polycrystal: application to third-order non-linear susceptibility*, J. Phys., Condens. Matter, 11 (1999), pp. 10323–10334.
- [6] D. J. BERGMAN, *The dielectric constant of a composite material – A problem in classical physics*, Phys. Rep. C, 43 (1978), pp. 377–407.
- [7] ———, *Exactly solvable microscopic geometries and rigorous bounds for the complex dielectric constant of a two-component composite material*, Phys. Rev. Lett., 44 (1980), pp. 1285–1287.
- [8] ———, *Rigorous bounds for the complex dielectric constant of a two-component composite*, Ann. Phys., 138 (1982), pp. 78–114.
- [9] C. BONIFASI-LISTA AND E. CHERKAEV, *Electrical impedance spectroscopy as a potential tool for recovering bone porosity*, Phys. Med. Biol., 54 (2009), pp. 3063–3082.
- [10] O. BRUNO, *The effective conductivity of strongly heterogeneous composites*, Proc. R. Soc. London A, 433 (1991), pp. 353–381.
- [11] O. BRUNO AND K. GOLDEN, *Interchangeability and bounds on the effective conductivity of the square lattice*, J. Stat. Phys., 61 (1990), pp. 365–386.
- [12] H. CHENG AND L. GREENGARD, *On the numerical evaluation of electrostatic fields in dense random dispersions of cylinders*, J. Comput. Phys., 136 (1997), pp. 629–639.
- [13] E. CHERKAEV, *Inverse homogenization for evaluation of effective properties of a mixture*, Inverse Problems, 17 (2001), pp. 1203–1218.
- [14] ———, *Spectral coupling of effective properties of a random mixture*, in IUTAM Symposium on Asymptotics, Singularities and Homogenisation in Problems of Mechanics, A. B. Movchan, ed., vol. 113 of Solid Mechanics and Its Applications, Springer Netherlands, 2004, pp. 331–340.
- [15] E. CHERKAEV AND C. BONIFASI-LISTA, *Characterization of structure and properties of bone by spectral measure method*, J. Biomech., 44 (2011), pp. 345–351.
- [16] E. CHERKAEV AND K. M. GOLDEN, *Inverse bounds for microstructural parameters of composite media derived from complex permittivity measurements*, Waves in Random Media, 8 (1998), pp. 437–450.
- [17] E. CHERKAEV AND M.-J. OU, *De-homogenization: Reconstruction of moments of the spectral measure of composite*, Inverse Problems, 24 (2008), p. 065008 (19pp.).
- [18] E. CHERKAEV AND D. ZHANG, *Coupling of the effective properties of a random mixture through the reconstructed spectral representation*, Physica B: Condensed Matter, 338 (2003), pp. 16–23.
- [19] R. W. R. DARLING, *Differential Forms and Connections*, Cambridge University Press, 1994.
- [20] A. R. DAY AND M. F. THORPE, *The spectral function of random resistor networks*, J. Phys., Condens. Matter, 8 (1996), pp. 4389–4409.
- [21] ———, *The spectral function of composites: the inverse problem*, J. Phys., Condens. Matter, 11 (1999), pp. 2551–2568.
- [22] P. DEIFT, *Orthogonal Polynomials and Random Matrices: a Riemann–Hilbert Approach*, Courant Institute of Mathematical Sciences, New York, NY, 2000.
- [23] J. W. DEMMEL, *Applied Numerical Linear Algebra*, SIAM, 1997.
- [24] N. DUNFORD AND J. T. SCHWARTZ, *Linear Operators, Part I*, John Wiley & Sons, Inc., Hoboken, NJ, 1988.
- [25] R. DURRETT, *Probability: Theory and Examples*, 4th Edition, Cambridge University Press, 2010.
- [26] G. B. FOLLAND, *Introduction to Partial Differential Equations*, Princeton University Press, Princeton, NJ, 1995.
- [27] ———, *Real Analysis: Modern Techniques and Their Applications*, Wiley–Interscience, New York, NY, 1999.
- [28] K. GOLDEN, *Bounds on the complex permittivity of a multicomponent material*, J. Mech. Phys. Solids, 34 (1986), pp. 333–358.
- [29] K. M. GOLDEN, *Exponent inequalities for the bulk conductivity of a hierarchical model*, Commun. Math. Phys., 143 (1992), pp. 467–499.

- [30] ———, *Statistical mechanics of conducting phase transitions*, J. Math. Phys., 36 (1995), pp. 5627–5642.
- [31] ———, *Critical behavior of transport in lattice and continuum percolation models*, Phys. Rev. Lett., 78 (1997), pp. 3935–3938.
- [32] ———, *The interaction of microwaves with sea ice*, in Wave Propagation in Complex Media, IMA Volumes in Mathematics and its Applications, Vol. 96, G. Papanicolaou, ed., Springer – Verlag, 1997, pp. 75–94.
- [33] K. M. GOLDEN, N. B. MURPHY, AND E. CHERKAEV, *Spectral analysis and connectivity of porous microstructures in bone*, J. Biomech., 44 (2011), pp. 337–344.
- [34] K. M. GOLDEN AND G. PAPANICOLAOU, *Bounds for effective parameters of heterogeneous media by analytic continuation*, Commun. Math. Phys., 90 (1983), pp. 473–491.
- [35] ———, *Bounds for effective parameters of multicomponent media by analytic continuation*, J. Stat. Phys., 40 (1985), pp. 655–667.
- [36] L. GREENGARD AND J.-Y. LEE, *Electrostatics and heat conduction in high contrast composite materials*, J. Comput. Phys., 211 (2006), pp. 64–76.
- [37] L. GREENGARD AND M. MOURA, *On the numerical evaluation of electrostatic fields in composite materials*, Acta Numerica, 3 (1994), pp. 379–410.
- [38] A. GULLY, J. LIN, E. CHERKAEV, AND K. M. GOLDEN, *Polycrystalline bounds on the complex permittivity of sea ice*. In Preparation, 2014.
- [39] P. R. HALMOS, *Finite Dimensional Vector Spaces*, Van Nostrand–Reinhold, Princeton, NJ, 1958.
- [40] J. HELSING, *The effective conductivity of arrays of squares: Large random unit cells and extreme contrast ratios.*, J. Comput. Phys., 230 (2011), pp. 7533–7547.
- [41] ———, *The effective conductivity of random checkerboards*, J. Comput. Phys., 230 (2011), pp. 1171–1181.
- [42] J. HELSING, R. C. MCPHEDRAN, AND G. W. MILTON, *Spectral super-resolution in metamaterial composites*, New J. Phys., 13 (2011), p. 115005 (17pp.).
- [43] J. HELSING AND R. OJALA, *Corner singularities for elliptic problems: Integral equations, graded meshes, quadrature, and compressed inverse preconditioning*, J. Comput. Phys., 227 (2008), pp. 8820–8840.
- [44] P. HENRICI, *Applied and Computational Complex Analysis. Volume 2.*, John Wiley & Sons Inc., New York, 1974.
- [45] R. A. HORN AND C. R. JOHNSON, *Matrix Analysis*, Cambridge University Press, 1990.
- [46] J. D. JACKSON, *Classical Electrodynamics*, John Wiley and Sons, Inc., New York, 1999.
- [47] T. JONCKHEERE AND J. M. LUCK, *Dielectric resonances of binary random networks*, J. Phys. A: Math. Gen., 31 (1998), pp. 3687–3717.
- [48] S. KARLIN AND W. J. STUDDEN, *Tchebycheff systems: with applications in analysis and statistics*, John Wiley & Sons, Inc., Hoboken, NJ, 1966.
- [49] J. P. KEENER, *Principles of applied mathematics: transformation and approximation*, Westview Press, Cambridge, MA, 2000.
- [50] J. B. KELLER, *A theorem on the conductivity of a composite medium*, J. Math. Phys., 5 (1964), pp. 548–549.
- [51] E. KREYSZIG, *Introductory functional analysis with applications*, John Wiley & Sons. Inc., New York, 1989.
- [52] D. McLAUGHLIN, G. PAPANICOLAOU, AND O. PIRONNEAU, *Convection of microstructure and related problems*, SIAM J. Appl. Math., 45 (1985), pp. 780–797.
- [53] R. C. MCPHEDRAN, D. R. MCKENZIE, AND G. W. MILTON, *Extraction of structural information from measured transport properties of composites*, Appl. Phys. A, 29 (1982), pp. 19–27.
- [54] R. C. MCPHEDRAN AND G. W. MILTON, *Inverse transport problems for composite media*, MRS Proceedings, 195 (1990).
- [55] G. W. MILTON, *Bounds on the complex dielectric constant of a composite material*, Appl. Phys. Lett., 37 (1980), pp. 300–302.
- [56] ———, *Bounds on the complex permittivity of a two component composite material*, J. Appl. Phys., 52 (1981), pp. 5286–5293.
- [57] ———, *Bounds on the transport and optical properties of a two-component composite material*, J. Appl. Phys., 52 (1981), pp. 5294–5304.
- [58] ———, *Theory of Composites*, Cambridge University Press, Cambridge, 2002.
- [59] N. B. MURPHY AND E. CHERKAEV, *Spectral analysis and computation for random polycrystalline media*. In Preparation, 2014.
- [60] N. B. MURPHY AND K. M. GOLDEN, *The Ising model and critical behavior of transport in binary composite media*, J. Math. Phys., 53 (2012), p. 063506 (25pp.).
- [61] ———, *Random matrix theory for phase transitions in composite media*. Submitted, 2014.

- [62] N. B. MURPHY, C. HOHENEGGER, C. S. SAMPSON, D. K. PEROVICH, H. EICKEN, E. CHERKAEV, B. ALALI, AND K. M. GOLDEN, *Spectral analysis of multiscale sea ice structures in the climate system*. In Preparation, 2014.
- [63] N. B. MURPHY, P. SHENG, AND K. M. GOLDEN, *Statistical mechanics of homogenization for composite media*. In Preparation, 2014.
- [64] N. B. MURPHY, J. XIN, E. CHERKAEV, AND J. ZHU, *Spectral theory of advective diffusion by steady and dynamic flows*. In Preparation, 2014.
- [65] N. B. MURPHY, J. ZHU, AND K. M. GOLDEN, *Spectral measure computations for advective diffusion by random flows*. In Preparation, 2014.
- [66] C. ORUM, E. CHERKAEV, AND K. M. GOLDEN, *Recovery of inclusion separations in strongly heterogeneous composites from effective property measurements*, Proc. Roy. Soc. London A, 468 (2012), pp. 784–809.
- [67] M. J. OU AND E. CHERKAEV, *On the integral representation formula for a two-component elastic composite*, Mathematical Methods in the Applied Sciences, 29 (2006), pp. 655–644.
- [68] M. Y. OU, *Two-parameter integral representation formula for the effective elastic moduli of two-phase composites.*, Complex Var. Elliptic Equ., 57 (2012), pp. 411–424.
- [69] G. PAPANICOLAOU AND S. VARADHAN, *Boundary value problems with rapidly oscillating coefficients*, in Colloquia Mathematica Societatis János Bolyai 27, Random Fields (Esztergom, Hungary 1979), North-Holland, 1982, pp. 835–873.
- [70] M. C. REED AND B. SIMON, *Functional Analysis*, Academic Press, San Diego CA, 1980.
- [71] W. RUDIN, *Real and Complex Analysis*, McGraw-Hill, Inc., New York, NY, 1987.
- [72] B. K. P. SCAIFE, *Principles of Dielectrics*, Clarendon Press, Oxford, 1989.
- [73] K. SCHULGASSER, *On the conductivity of fiber reinforced materials*, J. Math. Phys., 17 (1976), pp. 382–387.
- [74] J. A. SHOHAT AND J. D. TAMARKIN, *The Problem of Moments*, American mathematical society, Providence, RI, 1963.
- [75] L. B. SIMEONOVA, D. C. DOBSON, O. ESO, AND K. M. GOLDEN, *Spatial bounds on the effective complex permittivity for time-harmonic waves in random media*, Multiscale Modeling and Simulation, 9 (2011), pp. 1113–1143.
- [76] I. STAKGOLD, *Boundary Value Problems of Mathematical Physics: 2-Volume Set*, Classics in Applied Mathematics, SIAM, 2000.
- [77] D. STAUFFER AND A. AHARONY, *Introduction to Percolation Theory*, Taylor and Francis, London, second ed., 1992.
- [78] T.-J. STIELTJES, *Recherches sur les fractions continues*, Annales de la faculté des sciences de Toulouse, 4 (1995), pp. J1–J35.
- [79] M. H. STONE, *Linear Transformations in Hilbert Space*, American Mathematical Society, Providence, RI, 1964.
- [80] S. TORQUATO, *Random Heterogeneous Materials: Microstructure and Macroscopic Properties*, Springer-Verlag, New York, 2002.
- [81] D. ZHANG AND E. CHERKAEV, *Reconstruction of spectral function from effective permittivity of a composite material using rational function approximations*, J. Comput. Phys., 228 (2009), pp. 5390–5409.